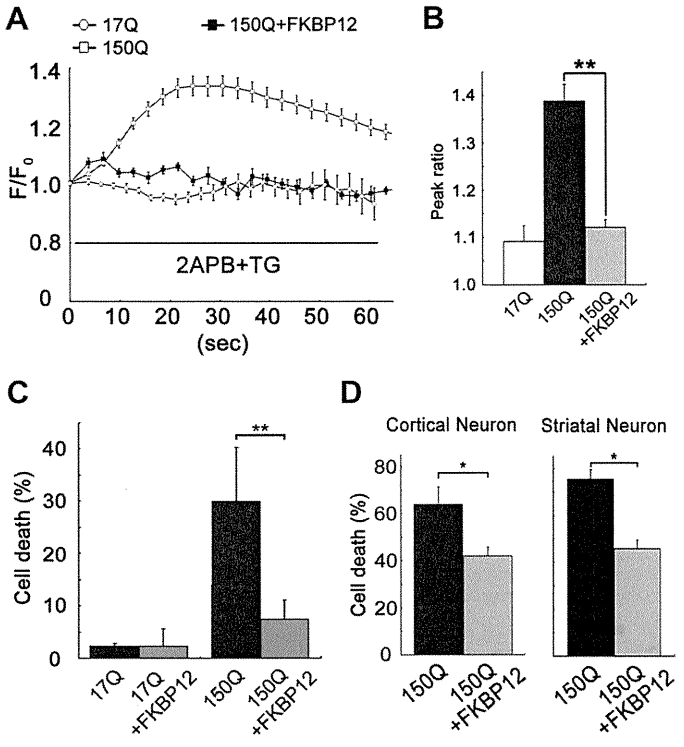

Fig. 4. Expression of RyR stabilizer FK506-binding protein 12 (FKBP12) suppresses mutant htt-induced abnormal Ca^{2+} leak and cell death. (A) Suppression of abnormal Ca^{2+} leak from RyR by FKBP12. HEK293t cells were co-transfected with RyR1 and BFP-tNhtt17Q (17Q), RyR1 and BFP-tNhtt150Q (150Q), or RyR1, BFP-tNhtt150Q and FKBP12 (150Q+FKBP12). Ca^{2+} leak was assessed at 48 h of transfection. The mean ± SE (n = 19–21). (B) Quantification of the results shown in A. (C) Suppression of mutant htt-induced cell death by FKBP12 in HEK 293t cells. Cell viability was evaluated 96 h after transfection. The mean ± SD (n = 3). (D) Attenuation of mutant htt-induced neuronal death by expression of FKBP12. Primary cultured cortical or striatal neurons were transfected for 96 h and cell viability was evaluated. The mean ± SD (n = 3). $^{*}p < 0.05$, $^{**}p < 0.01$.

To our knowledge, this study is the first report suggesting that Ca^{2+} leak through RyR contributes to pathogenesis of HD. Ca^{2+} leak from RyR1 has mainly been reported in muscular diseases such as malignant hyperthermia and muscular dystrophies. In these conditions, PKA (cAMP-dependent protein kinase)-dependent phosphorylation, oxidation or nitrosylation of RyR is shown to cause dissociation of FKBP proteins from the channels resulting in Ca^{2+} leak [25]. Although we have not assessed the status of RyR, there are several reports implicating that similar modification of RyR might be induced by mutant htt. For instance, increased activity of PKA [26] and nitric oxide synthase was found in R6/1 HD model mice [27] and increased reactive oxygen species and nitric oxide production was shown in a htt-expressing cellular model [28]. It has also been reported that FKBP12 mRNA level was decreased, whereas the expression of RyR1 increased, in caudate nucleus of grade 1 HD patient [23].

Then, how does Ca^{2+} leak induce neuronal cell death? Continuous Ca^{2+} leak might cause elevated cytosolic Ca^{2+} levels, which is observed in a YAC mouse model and R6/2 mouse [29,30]. Elevated cytosolic Ca^{2+} might lead mitochondrial depolarization through Ca^{2+} overload that cause energy disruption. Ca^{2+} overload also induces the release of cytochrome c that leads subsequent apoptotic pathways. It is reported that mitochondria of mutant htt-expressing cells show increased Ca^{2+} sensitivity of the permeability transition pore [12]. Not only mitochondrial damage, but also Ca^{2+} leak might amplify the toxicity of mutant htt in other ways. For example, elevated cytosolic Ca^{2+} may cause Calpain activation leading to generate toxic fragments [31]. Moreover, if the reduction in ER Ca^{2+} levels occurs, ER stress may be induced and eventually lead to cell death [32].

In addition to Ca^{2+} leak, we also found that caffeine-sensitive Ca^{2+} store might be depleted in mutant htt-expressing cells. Because Ca^{2+} leak was observed prior to declined caffeine responses in our cellular model (Figs. 3 and 4), continuous Ca^{2+} leak might result in Ca^{2+} depletion of caffeine-sensitive stores. Since RyR is considered to play a pivotal role in neuronal functions including excitation, neurotransmitter release, synaptic plasticity [33], stabilization of RyR might be effective not only in neuronal death but also in neuronal dysfunction of HD.

Currently there is no treatment for attenuating or reversing HD. Our results strongly indicate that dantrolene or other similar RyR inhibitors may be beneficial for HD patients. Notably, dantrolene is one of the clinically approved drugs and its neuroprotective effect has been shown in other neurological disease models including spinocerebellar ataxia type 2 and type 3, Alzheimer's disease and ischemia [9,10,14,15]. This study revealed novel mechanism of action whereby dantrolene attenuate neurodegeneration through suppression of Ca^{2+} leak from RyR and further support the notion that dantrolene should be potential therapeutic agent for the treatment of HD.

Acknowledgments

We would like to thank Dr. Nukina, Dr. Meissner and Dr. Miyazono for providing expression vectors. This work was supported by Hokkaido University Clark Memorial Foundation (MS), Core Research for Evolutional Science and Technology (CREST) of Japan Science and Technology Agency (YN) and a fund from the Japanese Ministry of Education, Culture, Sports, Science and Technology (TK). MS is an awardee of the fellowship by the COE program for Advance Life Science on the base of Bioscience and Nanotechnology Hokkaido University.

References

[1] P.O. Bauer, N. Nukina, The pathogenic mechanisms of polyglutamine diseases and current therapeutic strategies, J. Neurochem. 110 (2009) 1737–1765.
[2] J.P. Vonsattel, R.H. Myers, T.J. Stevens, R.J. Ferrante, E.D. Bird, E.P. Richardson Jr., Neuropathological classification of Huntington's disease, J. Neuropathol. Exp. Neurol. 44 (1985) 559–577.
[3] A. Lunkes, K.S. Lindenberg, L. Ben-Haiem, C. Weber, D. Devys, G.B. Landwehrmeyer, J.L. Mandel, Y. Trottier, Proteases acting on mutant huntingtin generate cleaved products that differentially build up cytoplasmic and nuclear inclusions, Mol. Cells 10 (2002) 259–269.
[4] Y. Nagai, H.A. Popiel, Conformational changes and aggregation of expanded polyglutamine proteins as therapeutic targets of the polyglutamine diseases: exposed beta-sheet hypothesis, Curr. Pharm. Des. 14 (2008) 3267–3279.
[5] I. Bezprozvanny, M.R. Hayden, Deranged neuronal calcium signaling and Huntington disease, Biochem. Biophys. Res. Commun. 322 (2004) 1310–1317.
[6] M. Suzuki, T. Koike, Early apoptotic and late necrotic components associated with altered Ca^{2+} homeostasis in a peptide-delivery model of polyglutamine-induced neuronal death, J. Neurosci. Res. 80 (2005) 549–561.
[7] M.P. Mattson, F.M. LaFerla, S.L. Chan, M.A. Leissring, P.N. Shepel, J.D. Geiger, Calcium signaling in the ER: its role in neuronal plasticity and neurodegenerative disorders, Trends Neurosci. 23 (2000) 222–229.
[8] T.S. Tang, H. Tu, E.Y. Chan, A. Maximov, Z. Wang, C.L. Wellington, M.R. Hayden, I. Bezprozvanny, Huntingtin and huntingtin-associated protein 1 influence neuronal calcium signaling mediated by inositol-(1,4,5) triphosphate receptor type 1, Neuron 39 (2003) 227–239.
[9] X. Chen, T.S. Tang, H. Tu, O. Nelson, M. Pook, R. Hammer, N. Nukina, I. Bezprozvanny, Deranged calcium signaling and neurodegeneration in spinocerebellar ataxia type 3, J. Neurosci. 28 (2008) 12713–12724.
[10] J. Liu, T.S. Tang, H. Tu, O. Nelson, E. Herndon, D.P. Huynh, S.M. Pulst, I. Bezprozvanny, Deranged calcium signaling and neurodegeneration in spinocerebellar ataxia type 2, J. Neurosci. 29 (2009) 9148–9162.
[11] X. Chen, J. Wu, S. Lvovskaya, E. Herndon, C. Supnet, I. Bezprozvanny, Dantrolene is neuroprotective in Huntington's disease transgenic mouse model, Mol. Neurodegener. 6 (2011) 81.
[12] D. Lim, L. Fedrizzi, M. Tartari, C. Zuccato, E. Cattaneo, M. Brini, E. Carafoli, Calcium homeostasis and mitochondrial dysfunction in striatal neurons of Huntington disease, J. Biol. Chem. 283 (2008) 5780–5789.

[13] P.O. Bauer, R. Hudec, S. Ozaki, M. Okuno, E. Ebisui, K. Mikoshiba, N. Nukina, Genetic ablation and chemical inhibition of IP3R1 reduce mutant huntingtin aggregation, Biochem. Biophys. Res. Commun. 416 (2011) 13–17.
[14] B. Oules, D. Del Prete, B. Greco, X. Zhang, I. Lauritzen, J. Sevalle, S. Moreno, P. Paterlini-Brechot, M. Trebak, F. Checler, F. Benfenati, M. Chami, Ryanodine receptor blockade reduces amyloid-beta load and memory impairments in Tg2576 mouse model of Alzheimer disease, J. Neurosci. 32 (2012) 11820–11834.
[15] F. Li, T. Hayashi, G. Jin, K. Deguchi, S. Nagotani, I. Nagano, M. Shoji, P.H. Chan, K. Abe, The protective effect of dantrolene on ischemic neuronal cell death is associated with reduced expression of endoplasmic reticulum stress markers, Brain Res. 1048 (2005) 59–68.
[16] S. Muehlschlegel, J.R. Sims, Dantrolene: mechanisms of neuroprotection and possible clinical applications in the neurointensive care unit, Neurocrit. Care 10 (2009) 103–115.
[17] G.H. Wang, K. Mitsui, S. Kotliarova, A. Yamashita, Y. Nagao, S. Tokuhiro, T. Iwatsubo, I. Kanazawa, N. Nukina, Caspase activation during apoptotic cell death induced by expanded polyglutamine in N2a cells, Neuroreport 10 (1999) 2435–2438.
[18] L. Gao, A. Tripathy, X. Lu, G. Meissner, Evidence for a role of C-terminal amino acid residues in skeletal muscle Ca^{2+} release channel (ryanodine receptor) function, FEBS Lett. 412 (1997) 223–226.
[19] T. Okadome, E. Oeda, M. Saitoh, H. Ichijo, H.L. Moses, K. Miyazono, M. Kawabata, Characterization of the interaction of FKBP12 with the transforming growth factor-beta type I receptor in vivo, J. Biol. Chem. 271 (1996) 21687–21690.
[20] M. Jiang, L. Deng, G. Chen, High Ca(2+)-phosphate transfection efficiency enables single neuron gene analysis, Gene Ther. 11 (2004) 1303–1311.
[21] X. Liu, M.J. Betzenhauser, S. Reiken, A.C. Meli, W. Xie, B.X. Chen, O. Arancio, A.R. Marks, Role of leaky neuronal ryanodine receptors in stress- induced cognitive dysfunction, Cell 150 (2012) 1055–1067.
[22] F. Zhao, P. Li, S.R. Chen, C.F. Louis, B.R. Fruen, Dantrolene inhibition of ryanodine receptor Ca^{2+} release channels molecular mechanism and isoform selectivity, J. Biol. Chem. 276 (2001) 13810–13816.
[23] A. Hodges, A.D. Strand, A.K. Aragaki, A. Kuhn, T. Sengstag, G. Hughes, L.A. Elliston, C. Hartog, D.R. Goldstein, D. Thu, Z.R. Hollingsworth, F. Collin, B. Synek, P.A. Holmans, A.B. Young, N.S. Wexler, M. Delorenzi, C. Kooperberg, S.J. Augood, R.L. Faull, J.M. Olson, L. Jones, R. Luthi-Carter, Regional and cellular gene expression changes in human Huntington's disease brain, Hum. Mol. Genet. 15 (2006) 965–977.
[24] A.B. Brillantes, K. Ondrias, A. Scott, E. Kobrinsky, E. Ondriasova, M.C. Moschella, T. Jayaraman, M. Landers, B.E. Ehrlich, A.R. Marks, Stabilization of calcium release channel (ryanodine receptor) function by FK506-binding protein, Cell 77 (1994) 513–523.
[25] S.E. Lehnart, Novel targets for treating heart and muscle disease: stabilizing ryanodine receptors and preventing intracellular calcium leak, Curr. Opin. Pharmacol. 7 (2007) 225–232.
[26] A. Giralt, A. Saavedra, O. Carreton, X. Xifro, J. Alberch, E. Perez-Navarro, Increased PKA signaling disrupts recognition memory and spatial memory: role in Huntington's disease, Hum. Mol. Genet. 20 (2011) 4232–4247.
[27] F. Perez-Severiano, B. Escalante, P. Vergara, C. Rios, J. Segovia, Age-dependent changes in nitric oxide synthase activity and protein expression in striata of mice transgenic for the Huntington's disease mutation, Brain Res. 951 (2002) 36–42.
[28] W.J. Firdaus, A. Wyttenbach, P. Giuliano, C. Kretz-Remy, R.W. Currie, A.P. Arrigo, Huntingtin inclusion bodies are iron-dependent centers of oxidative events, FEBS J. 273 (2006) 5428–5441.
[29] J.G. Hodgson, N. Agopyan, C.A. Gutekunst, B.R. Leavitt, F. LePiane, R. Singaraja, D.J. Smith, N. Bissada, K. McCutcheon, J. Nasir, L. Jamot, X.J. Li, M.E. Stevens, E. Rosemond, J.C. Roder, A.G. Phillips, E.M. Rubin, S.M. Hersch, M.R. Hayden, A YAC mouse model for Huntington's disease with full-length mutant huntingtin, cytoplasmic toxicity, and selective striatal neurodegeneration, Neuron 23 (1999) 181–192.
[30] O. Hansson, E. Guatteo, N.B. Mercuri, G. Bernardi, X.J. Li, R.F. Castilho, P. Brundin, Resistance to NMDA toxicity correlates with appearance of nuclear inclusions, behavioural deficits and changes in calcium homeostasis in mice transgenic for exon 1 of the Huntington gene, Eur. J. Neurosci. 14 (2001) 1492–1504.
[31] J. Gafni, L.M. Ellerby, Calpain activation in Huntington's disease, J. Neurosci. 22 (2002) 4842–4849.
[32] H.N. Nguyen, C. Wang, D.C. Perry, Depletion of intracellular calcium stores is toxic to SH-SY5Y neuronal cells, Brain Res. 924 (2002) 159–166.
[33] S. Bardo, M.G. Cavazzini, N. Emptage, The role of the endoplasmic reticulum Ca^{2+} store in the plasticity of central neurons, Trends Pharmacol. Sci. 27 (2006) 78–84.

Knockdown of the *Drosophila* Fused in Sarcoma (FUS) Homologue Causes Deficient Locomotive Behavior and Shortening of Motoneuron Terminal Branches

Hiroshi Sasayama[1☯], Mai Shimamura[2,3☯], Takahiko Tokuda[1,4*], Yumiko Azuma[1], Tomokatsu Yoshida[1], Toshiki Mizuno[1], Masanori Nakagawa[1], Nobuhiro Fujikake[5], Yoshitaka Nagai[5], Masamitsu Yamaguchi[2,3*]

1 Department of Neurology, Graduate School of Medical Science, Kyoto Prefectural University of Medicine, Kamigyo-ku, Kyoto, Japan, **2** Department of Applied Biology, Kyoto Institute of Technology, Matsugasaki, Sakyo-ku, Kyoto, Japan, **3** Insect Biomedical Research Center, Kyoto Institute of Technology, Matsugasaki, Sakyo-ku, Kyoto, Japan, **4** Department of Molecular Pathobiology of Brain Diseases, Graduate School of Medical Science, Kyoto Prefectural University of Medicine, Kamigyo-ku, Kyoto, Japan, **5** Department of Degenerative Neurological Diseases, National Institute of Neuroscience, National Center of Neurology and Psychiatry, Kodaira, Tokyo, Japan

Abstract

Mutations in the fused in sarcoma/translated in liposarcoma gene (FUS/TLS, FUS) have been identified in sporadic and familial forms of amyotrophic lateral sclerosis (ALS). FUS is an RNA-binding protein that is normally localized in the nucleus, but is mislocalized to the cytoplasm in ALS, and comprises cytoplasmic inclusions in ALS-affected areas. However, it is still unknown whether the neurodegeneration that occurs in ALS is caused by the loss of FUS nuclear function, or by the gain of toxic function due to cytoplasmic FUS aggregation. Cabeza (Caz) is a *Drosophila* orthologue of human FUS. Here, we generated *Drosophila* models with *Caz* knockdown, and investigated their phenotypes. In wild-type *Drosophila*, Caz was strongly expressed in the central nervous system of larvae and adults. Caz did not colocalize with a presynaptic marker, suggesting that Caz physiologically functions in neuronal cell bodies and/or their axons. Fly models with neuron-specific *Caz* knockdown exhibited reduced climbing ability in adulthood and anatomical defects in presynaptic terminals of motoneurons in third instar larvae. Our results demonstrated that decreased expression of *Drosophila* Caz is sufficient to cause degeneration of motoneurons and locomotive disability in the absence of abnormal cytoplasmic Caz aggregates, suggesting that the pathogenic mechanism underlying FUS-related ALS should be ascribed more to the loss of physiological FUS functions in the nucleus than to the toxicity of cytoplasmic FUS aggregates. Since the *Caz*-knockdown *Drosophila* model we presented recapitulates key features of human ALS, it would be a suitable animal model for the screening of genes and chemicals that might modify the pathogenic processes that lead to the degeneration of motoneurons in ALS.

Citation: Sasayama H, Shimamura M, Tokuda T, Azuma Y, Yoshida T, et al. (2012) Knockdown of the *Drosophila* Fused in Sarcoma (FUS) Homologue Causes Deficient Locomotive Behavior and Shortening of Motoneuron Terminal Branches. PLoS ONE 7(6): e39483. doi:10.1371/journal.pone.0039483

Editor: Koichi M. Iijima, Thomas Jefferson University, United States of America

Received January 9, 2012; **Accepted** May 21, 2012; **Published** June 19, 2012

Funding: TT is supported by Grants-in-Aid from the Research Committee of CNS Degenerative Diseases, the Ministry of Health, Labour and Welfare of Japan. The funders had no role in study design, data collection and analysis, decision to publish, or preparation of the manuscript.

Competing Interests: The authors have declared that no competing interests exist.

* E-mail: ttokuda@koto.kpu-m.ac.jp (TT); myamaguc@kit.ac.jp (MY)

☯ These authors contributed equally to this work.

Introduction

Amyotrophic lateral sclerosis (ALS) is a devastating neurodegenerative disease that is characterized by degeneration of motor neurons, which leads to progressive muscle weakness and eventually fatal paralysis, typically within 1 to 5 years after disease onset [1]. Frontotemporal lobar degeneration (FTLD) is a clinically diverse dementia syndrome, with phenotypes that include behavioral changes, semantic dementia and progressive non-fluent aphasia [2]. Although these two diseases are clinically distinct and affect different parts of the central nervous system, it has been long thought that these two diseases are related since ALS patients often develop cognitive deficits with frontotemporal features and FTLD patients can present symptoms of motor neuron disease [3,4]. This hypothesis, which was derived from clinical observations, has been biochemically confirmed by identification of the 43 kDa TAR-DNA-binding protein (TDP-43) as the major aggregating protein in subtypes of both ALS and FTLD (ALS-TDP and FTLD-TDP, respectively) [5,6]. Moreover, over 30 different mutations in the TDP-43 gene (*TARDBP*) have been identified in various sporadic and familial ALS patients [7–12], and subsequently TDP-43 mutations were reported in various FTLD-TDP cases [13,14]. Shortly after the identification of mutations in TDP-43 in ALS cases, mutations in another gene encoding an RNA-binding protein, FUS (fused in sarcoma; also known as TLS, translocated in liposarcoma), were identified in cases with familial ALS (ALS-FUS) [15,16]. Both dominantly and recessively inherited *FUS* mutations have been reported in familial ALS [15], and *FUS* mutations may be more common than *TARDBP* mutations in familial ALS [17]. Additional mutations in *FUS* have recently been identified in sporadic ALS cases and in a subset of FTLD cases (FTLD-FUS) [18,19]. FUS is normally a nuclear protein, but cytoplasmic FUS-immunoreactive inclusions were demonstrated in lower motor neurons of ALS patients

harboring *FUS* mutations [16]. Cytoplasmic aggregation of wild-type FUS was subsequently reported as the prominent disease phenotype in other neurodegenerative diseases such as basophilic inclusion body disease [20], some types of juvenile ALS [21], and in the majority of tau- and TDP43-negative FTLD [22]. The identification of these two RNA-binding proteins that aggregate and are sometimes mutated in ALS and FTLD gave rise to the emerging concept that disturbances in RNA regulation may play a major role in the pathogenesis of ALS and FTLD [23]. Moreover, FUS aggregation is also demonstrated in Huntington's disease, spinocerebellar ataxia types 1, 2, and 3, and dentatorubropallidoluysian atrophy [24,25]. These findings suggest an important role for FUS aggregation in the pathogenesis of neurodegenerative diseases beyond ALS and FTLD.

FUS is a ubiquitously expressed, 526 amino acid protein that was initially identified as a proto-oncogene, and which causes liposarcoma due to chromosomal translocation [26]. FUS is an RNA-binding protein that is implicated in multiple aspects of RNA metabolism including microRNA processing, RNA splicing, trafficking and translation [23,27,28]. FUS shows nuclear and cytoplasmic expression and shuttles between the nucleus and the cytoplasm [27,29]. In neurons, FUS is localized to the nucleus but it is transported to dendritic spines at excitatory post-synapses in a complex with RNA and other RNA-binding proteins [30]. Similar to TDP-43, FUS comprises a glycine-rich domain (GRD), an RNA-recognition-motif (RRM) domain and a nuclear localization sequence (NLS). ALS/FTLD-associated mutations cluster in the C-terminal region of the FUS protein that contains a non-classical R/H/KX$_{2-5}$PY NLS motif [31] as well as in the GRD motif that is important for protein-protein interactions and also exists in the C-terminal region of TDP-43. Most pathogenic mutations of the *TARDBP* gene cluster in this GRD motif. The only known genetic cause for ALS/FTLD with FUS pathology is mutations in the *FUS* gene itself. The *FUS* mutations in the NLS-containing C-terminal region lead to redistribution of the FUS protein from the nucleus to the cytoplasm [32–35]. These findings suggest that the loss of physiological nuclear functions of FUS that involve RNA regulation may contribute to the pathogenesis of ALS/FTLD.

There is a single homolog for each of human FUS and TDP-43 in *Drosophila*, named Cabeza (Caz) and TBPH, respectively. The *Caz* gene is located on the X chromosome, and is a member of an RNA binding proteins that are conserved from fly to man. *In situ* hybridization and immunohistochemical analyses demonstrated that Caz mRNA and protein are enriched in the brain and CNS during embryogenesis, and the Caz protein was detected in the nuclei of several larval tissues and in imaginal discs [36]. The full-length recombinant Caz protein and its RRM domain are capable of binding RNA in vitro [36]. These findings suggest that Caz is a nuclear RNA binding protein that may play an important role in the regulation of RNA metabolism during fly development. Feiguin et al. reported that *Drosophila* lacking TBPH presented deficient locomotive behaviors, reduced life span and anatomical defects at neuromuscular junctions (NMJ), suggesting that a loss of TDP-43 nuclear functions could be a causative factor of the neurodegeneration observed in patients with ALS/FTLD [37].

As mentioned above, the loss of the nuclear function of FUS or TDP-43 plays an important role in the pathogenesis of ALS/FTLD. However, aggregation of TDP-43 or FUS may by itself be toxic due to a toxic gain-of-function associated with the formation of cytoplasmic aggregates of those proteins, which would trap vital proteins and/or RNAs and might disturb cellular homeostasis. Thus, it remains unclear whether it is the loss of FUS nuclear function or the gain of toxic function resulting from FUS aggregation that is the mechanism that underlies the primary abnormality that leads to the neurodegeneration that occurs in ALS/FTLD. The existence of both dominantly and recessively inherited *FUS* mutations in familial ALS has provoked further controversy regarding whether the underlying pathogenic mechanism of ALS/FTLD is due to gain-of-toxic-function or loss-of-nuclear function [15,19,38]. Here, we investigated phenotypes of fly models with knockdown of the *Drosophila* FUS homologue, *Caz* gene, to provide supporting evidence for our hypothesis that the pathogenesis of ALS/FTLD may be due more to the loss of physiological FUS functions than to the toxicity of its cytoplasmic aggregates. Neuron-specific knockdown of the *Drosophila Caz* gene reduced the climbing abilities of adult flies as well as caused anatomical defects, such as a reduced length of synaptic branches, in presynaptic terminals of motoneurons in third instar larvae, suggesting that decreased expression of the *Drosophila* FUS homologue may be sufficient for development of the degeneration of motoneurons and for the deficient locomotive behavior in this model fly.

Results

Comparison of the amino acid sequence of human FUS and *Drosophila* Caz

The amino acid sequence of *Drosophila* Caz was retrieved from the Flybase and was compared with that of human FUS using BLAST and FASTA (Figure 1). The identity and the similarity of the amino acid sequences of Caz and FUS are 44.9% and 62.3%, respectively. Regarding conservation of specific FUS domains, the RRM domain, which is known to bind RNAs, as well as the zinc finger domain, are both highly conserved between human FUS and *Drosophila* Caz, showing 50% and 63% identity, respectively. The similarity of the human and *Drosophila* RRM and zinc finger domains is as high as 75% and 73%, respectively.

Specificity of the anti-Caz antibody

We raised a polyclonal antibody against a mixed peptide corresponding to residues 30–45 and 382–390 of *Drosophila* Caz for immunological studies. In order to confirm the specificity of this antibody, we used this anti-Caz polyclonal antibody for immunoblotting analyses of CNS extracts of third instar larvae carrying *elav^{3A}-GAL4/+* (*elav^{3A}/+*, a driver control fly), *UAS-Caz-IR/+* (a responder control fly), and RNAi transgenes encoding inverted repeats corresponding to various Caz regions, *elav^{3A}-GAL4>UAS-Caz-IR* (Figure 2). A single major band with an apparent molecular weight of 45 kDa was detected on immunoblots of all of the flies using the anti-Caz antibody (Figure 2A). Although the size of this protein was slightly larger than the size (38.8 kDa) of the Caz protein predicted based on its amino acid composition, the intensity of this band was significantly reduced in flies carrying *elav^{3A}-GAL4>UAS-Caz-IR$_{1-167}$* (*elav^{3A}/Caz-IR$_{1-167}$*) and those carrying *elav^{3A}-GAL4>UAS-Caz-IR$_{363-399}$* (*Caz-IR$_{363-399}$/+;elav^{3A}/+*) compared with its intensity in either driver control flies (*elav^{3A}/+*) or responder control flies (*UAS-Caz-IR$_{1-167}$/+*) (Figure 2B). There was a significant increase in Caz protein level in CNS extracts from the flies carrying *elav^{3A}/Caz-IR$_{180-346}$* compared with those from control flies carrying *elav^{3A}/+* with unknown causes (Figure 2B). These results indicate that the anti-Caz antibody can specifically detect the Caz protein. These data also confirmed that *Caz* is effectively knocked down in flies carrying *elav^{3A}/Caz-IR$_{1-167}$* and *Caz-IR$_{363-399}$/+;elav^{3A}/+*, but it is not knocked down in flies carrying *elav^{3A}-GAL4>UAS-Caz-IR$_{180-346}$*, which we did not therefore use in the subsequent experiments.

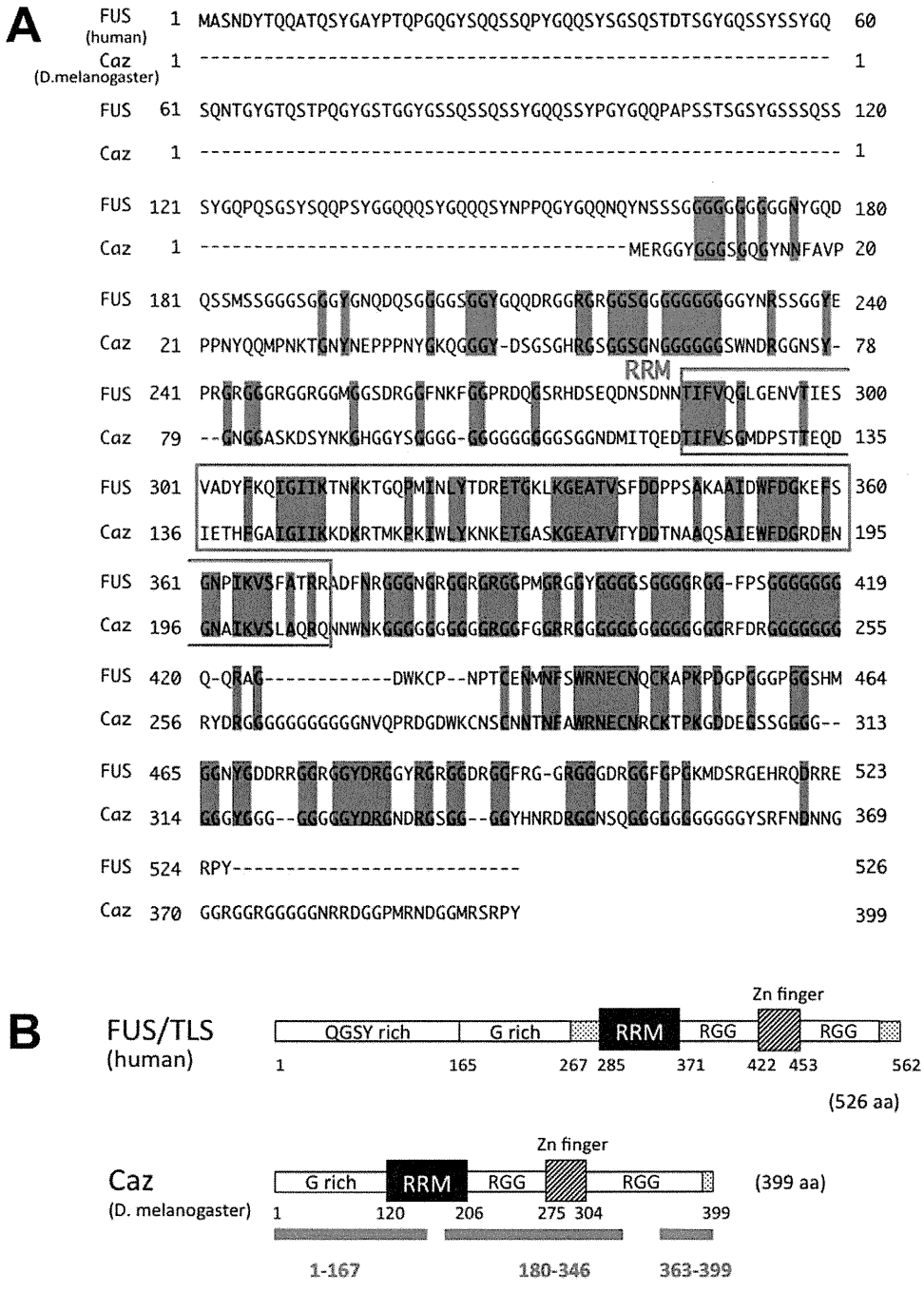

Figure 1. Comparison of human FUS and *Drosophila* Caz. (A) Alignment of human FUS and *Drosophila* Caz amino acid sequences. Identity is indicated in blue. The RNA-recognition-motif (RRM) domain is outlined with a red box. (B) Schematic drawings of domain structures of Human FUS and *Drosophila* Caz proteins. The human FUS protein contains an N-terminal QGSY-rich domain, which functions as a potent transcriptional activation domain [62–64]. The glycine-rich domain (G rich), RRM domain, a domain containing multiple Arg-Gly-Gly (RGG) motifs and a zinc finger (ZnF), are all involved in RNA binding [65,66]. A solid line under the schema of *Drosophila* Caz shows the target genomic sequence of each of the three RNAi transgenes employed in this study, *UAS-Caz-IR*$_{1-167}$, *UAS-Caz-IR*$_{180-346}$ and *UAS-Caz-IR*$_{363-399}$.
doi:10.1371/journal.pone.0039483.g001

The Caz protein is localized in the larval and adult central nervous system of *Drosophila*

The polyclonal anti-Caz antibody was used to examine the expression pattern of the Caz protein in the CNS of third instar *Drosophila* larvae and adult flies (Figure 3). *Drosophila* Caz was strongly expressed in the CNS of both larvae (Figure 3, A1) and adults (Figure 3, E1). No signal was generated in the absence of the primary anti-Caz antibody (Figure 3, D, H) indicating that this signal is specific for detection of the Caz protein. Moreover, the anti-Caz antibody signal did not overlap with the signal of the presynaptic marker Bruchpilot (Brp) that was detected using an anti-Brp antibody (Figure 3, A3-A4, E3-E4). This finding indicates that Caz localizes in a region other than synaptic areas both in third instar larvae and in adult flies (Figure 3, A1-A4, E1-E4), and

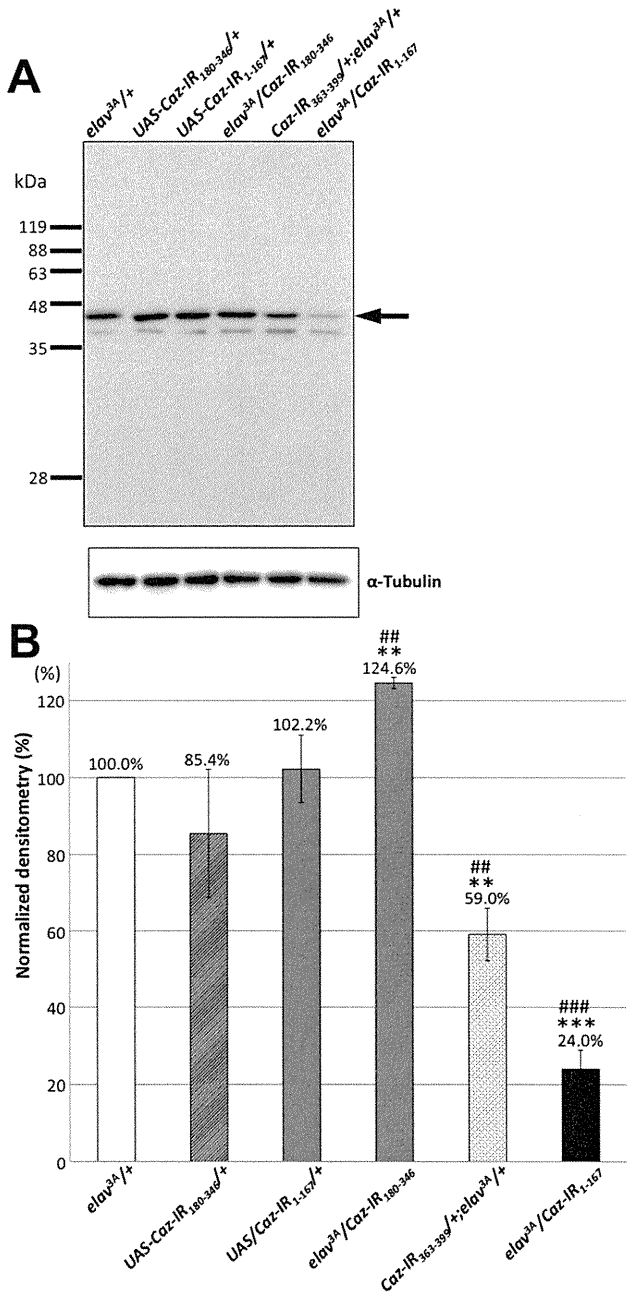

Figure 2. Western immunoblot analysis of the CNS extracts of third instar larvae. (A) A representative result of the analysis of protein extracts from the CNS of the driver control (*elav^{3A}*/+) and responder control (*UAS-Caz-IR$_{180-346}$*/+ and *UAS-Caz-IR$_{1-167}$*/+) flies (n = 5, each) and transgenic flies (*elav^{3A}/Caz-IR$_{180-346}$*, *Caz-IR$_{363-399}$*/+;*elav^{3A}*/+ and *elav^{3A}/Caz-IR$_{1-167}$*) (n = 5, each). The blots were probed with the polyclonal anti-Caz antibody that was newly raised for this study. α-Tubulin was used as a loading control. A 45-kDa band (arrow) corresponds to the Caz protein. (B) Densitometric quantification of the 45-kDa bands derived from triplicated immunoblot analyses of the CNS tissues of each fly strain in (A). The intensity of the 45 kDa band which indicates the expression level of Caz protein was much weaker in flies carrying *elav^{3A}/Caz-IR$_{1-167}$* or *Caz-IR$_{363-399}$*/+;*elav^{3A}*/+ than in the driver and responder control flies. The columns and horizontal bars indicate the mean values and the standard errors of the triplicated experiments. **p<0.01 (vs. *elav^{3A}*/+), *** p<0.001 (vs. *elav^{3A}*/+), ##p<0.01 (vs. *UAS-Caz-IR$_{1-167}$*/+), ###p<0.001 (vs. *UAS-Caz-IR$_{1-167}$*/+).
doi:10.1371/journal.pone.0039483.g002

suggests that Caz performs its physiological functions in neuronal cell bodies and/or their axons.

Regarding the precise localization of the Caz protein in neuronal cell bodies, Caz immunoreactivity was detected in the nucleus of neuronal cells of third instar larvae and did not co-localize with actin filaments, which are cytosolic proteins (Figure 4). However, within the nucleus, Caz did not co-localize with diamino-2-phenylidole (DAPI), suggesting that Caz is not localized on chromosomes but is localized in the nucleoplasm (Figure 4, C and D).

Neuron-specific *Caz* knockdown causes fly mobility defects

To analyze the effect of *Caz* knockdown on fly phenotypes, we first investigated whether fly viability was affected by whole-body knockdown of *Caz*. Using an *Act5C-GAL4* driver that expresses GAL4 in the whole body of the fly, we analyzed the phenotypes of flies in which *Caz* double-stranded RNA was expressed throughout the whole body (Table 1). When crossed at 28°C, *UAS-Caz-IR$_{1-167}$* was lethal at the pupal stage for all fly strains that carried it, while the strains carrying *UAS-Caz-IR$_{180-346}$* were viable. When crossed at 25°C to decrease the expression levels of *Act5C-GAL4*, almost all of the strains carrying *UAS-Caz-IR$_{1-167}$*, for which *UAS-Caz-IR$_{1-167}$* had been lethal when crossed at 28°C, changed to be viable.

We next established transgenic fly lines in which *Caz* double-stranded RNA was specifically expressed in neuronal tissue by crossing the transgenic flies with the *elav^{3A}-GAL4* line. As shown above in the immunoblotting analyses of the fly CNS (Figure 2), the expression levels of the Caz protein were much decreased in strain 3 of the fly lines that carried *elav^{3A}/Caz-IR$_{1-167}$* and in the fly line carrying *Caz-IR$_{363-399}$*/+;*elav^{3A}*/+, compared with the control flies. However, Caz expression levels did not show any detectable decreases in the fly lines carrying *elav^{3A}-GAL4>UAS-Caz-IR$_{180-346}$*. Similar to these results of immunoblotting analyses, immunostaining of the CNS of third instar larvae (Figure 3, B1, C1) and adult flies (Figure 3, F1, G1) showed that immunoreactivity detected with the anti-Caz antibody also decreased in the CNS tissues derived from the fly lines carrying *elav^{3A}/Caz-IR$_{1-167}$* (strain 3) (Figure 3, B1: larva, F1: adult fly) and *Caz-IR$_{363-399}$*/+;*elav^{3A}*/+ (Figure 3, C1: larva, G1: adult fly). These results confirmed that *Caz* is effectively knocked down in the CNS of those two lines of transgenic flies.

To examine the effects of neuron-specific *Caz*-knockdown on the fly life span, we next determined the life span of each genotype (Figure 5). We examined adult flies until 120 days after eclosion, but there were no significant differences in life span between the control flies carrying *elav^{3A}*/+ (n = 145) and those carrying *elav^{3A}/Caz-IR$_{1-167}$* (n = 144) or *Caz-IR$_{363-399}$*/+;*elav^{3A}*/+ (n = 161), in which the CNS expression of Caz was efficiently knocked down (Figure 5). The average life span of the control flies was 73.9 days, whereas flies carrying *elav^{3A}/Caz-IR$_{1-167}$* and *Caz-IR$_{363-399}$*/+;*elav^{3A}*/+ lived an average of 76.5 days and 70.7 days, respectively. Fly life spans were therefore not significantly different between the control and neuron-specific *Caz*-knockdown flies.

In order to further evaluate the functional effects of neuron-specific *Caz* knockdown, we then performed climbing assays of the *Caz*-knockdown fly strains (Figure 6). The flies carrying *elav^{3A}/Caz-IR$_{1-167}$* showed reduced mobility both on day 3 (−10.7%) and day 21 (−9.3%) compared to the control flies carrying *elav^{3A}*/+. Similarly *Caz-IR$_{363-399}$*/+;*elav^{3A}*/+ carrying flies showed reduced mobility both on day 3 (−5.1%) and on day 21 (−10.6%). All of these reductions in mobility were statistically significant (p<0.001). These results indicate that *Caz* is involved in locomotion.

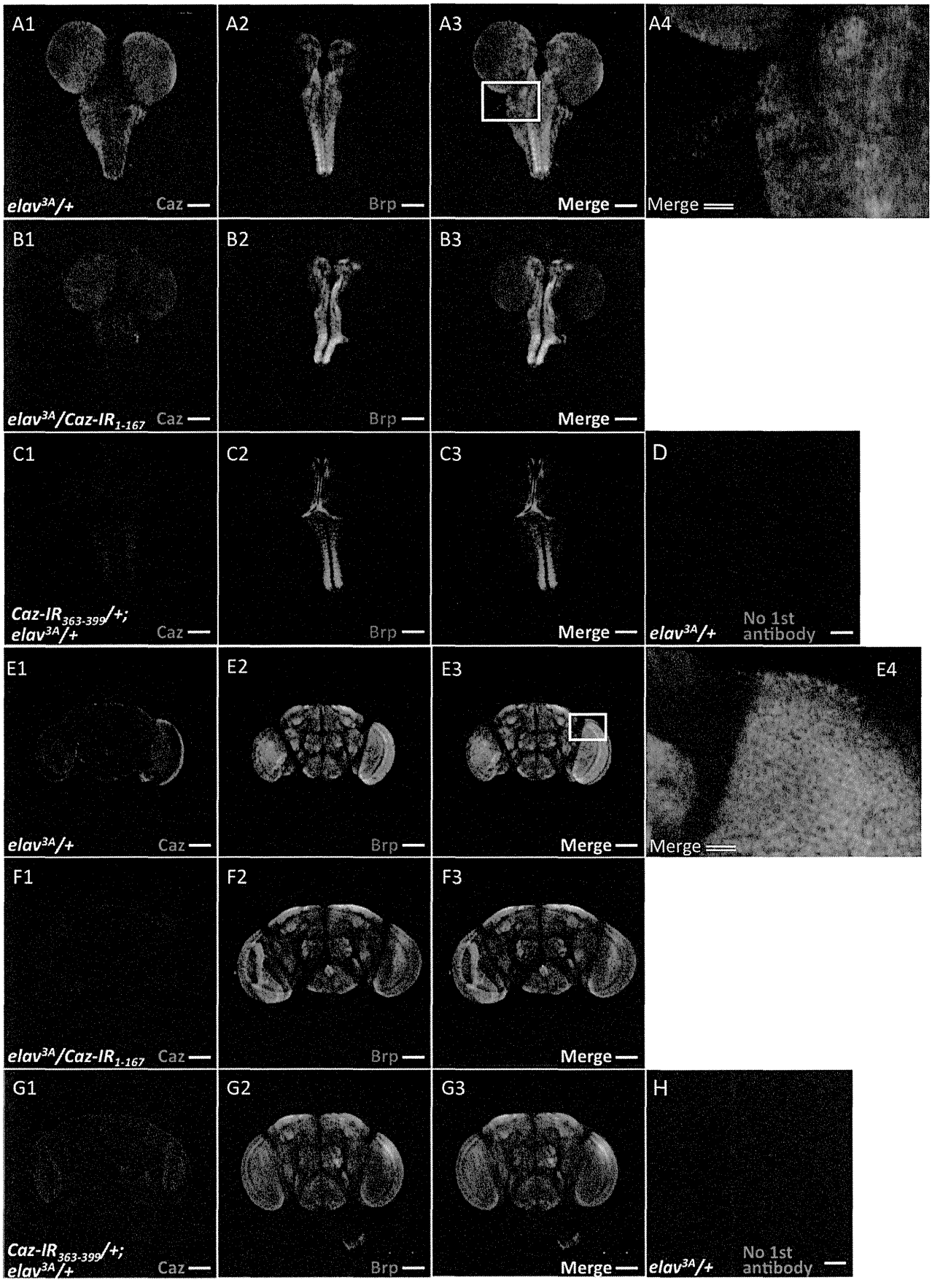
A1
A2
A3
A4
elav3A/+
Caz
Brp
Merge
Merge
B1
B2
B3
elav3A/Caz-IR1-167
Caz
Brp
Merge
C1
C2
C3
D
Caz-IR363-399/+;
elav3A/+
Caz
Brp
Merge
elav3A/+
No 1st
antibody
E1
E2
E3
E4
elav3A/+
Caz
Brp
Merge
Merge
F1
F2
F3
elav3A/Caz-IR1-167
Caz
Brp
Merge
G1
G2
G3
H
Caz-IR363-399/+;
elav3A/+
Caz
Brp
Merge
elav3A/+
No 1st
antibody

Figure 3. Immunohistochemical localization of Caz in larval and adult brains. Brain-ventral ganglia complexes from third instar larvae (A–D) and whole mount adult heads (E–H) were stained with the polyclonal anti-Caz antibody (A-1, B-1, C-1, E-1, F-1, G-1) or with an antibody against the neuropil marker Bruchpilot (Brp) (A-2, B-2, C-2, E-2, F-2, G-2). Merged confocal images of the two stains are shown at right (A-3, B-3, C-3, E-3, F-3 and G-3, respectively). Higher-magnification images of the boxed area in A-3 and E-3 are shown in A-4 and E-4, respectively. (D, H) Images of staining in the absence of first antibody. A-1 to A-4, E-1 to E-4, controls carrying $elav^{3A}$/+; B-1 to B-3, F-1 to F-3, *Caz*-knockdown flies carrying $elav^{3A}$/*Caz-IR*$_{1\text{-}167}$; C-1 to C-3, G-1 to G-3, *Caz*-knockdown flies carrying *Caz-IR*$_{363\text{-}399}$/+;$elav^{3A}$/+. Caz antibody immunoreactivity decreased in CNS tissues from both the third instar larvae and the adult flies carrying $elav^{3A}$/*Caz-IR*$_{1\text{-}167}$ (B-1, F-1) and *Caz-IR*$_{363\text{-}399}$/+;$elav^{3A}$/+ (C-1, G-1). The single bars indicate 100 μm. The double bars indicate 20 μm.
doi:10.1371/journal.pone.0039483.g003

Caz regulates the formation of motoneurons at presynaptic terminals in the NMJ

Based on the fact that *Caz*-knockdown flies showed motor deficits in the climbing assays, together with the fact that *FUS*, the human counterpart of *Caz*, is involved in ALS that impairs motor neurons, we therefore decided to analyze the morphology of motoneuron presynaptic terminals at NMJs in these flies. Because most motoneurons of the adult fly originate from larval motoneurons, we compared the NMJ structure of the larvae of $elav^{3A}$/*Caz-IR*$_{1\text{-}167}$ and *Caz-IR*$_{363\text{-}399}$/+;$elav^{3A}$/+ flies with that of larvae of control flies carrying $elav^{3A}$/+ or *UAS-Caz-IR*$_{363\text{-}399}$/+. None of these *Caz*-knockdown fly larvae showed apparent changes in NMJ structure (Figure 7, A-D). However, measurement of the total length of synaptic branches of motoneurons in these larvae indicated that the total branch length was significantly decreased in $elav^{3A}$/*Caz-IR*$_{1\text{-}167}$ (75.3±11.9 μm) and *Caz-IR*$_{363\text{-}399}$/+;$elav^{3A}$/+ (75.3±19.5 μm) flies compared to that of the both driver ($elav^{3A}$/+; 94.8±19.9 μm) and responder (*UAS-Caz-IR*$_{363\text{-}399}$/+; 105.4±17.5 μm) control *flies*. (Figure 7, E). The flies carrying $elav^{3A}$/*Caz-IR*$_{1\text{-}167}$ showed the significantly decreased number of the synaptic boutons (9.3±2.1) compared to the both driver (15.9±4.5) and responder (17.1±4.7) control flies, and so did the flies carrying *Caz-IR*$_{363\text{-}399}$/+;$elav^{3A}$/+ (11.8±5.6) compared to the responder controls (Figure 7, F). There were no significant differences in the size of synaptic boutons among those 4 genotypes (Figure 7, G). These results indicate that Caz is required for synaptic terminal growth at the NMJ.

Discussion

We showed here that *Drosophila* Caz is strongly expressed in the central nervous system of larvae and adults. Caz did not colocalize with the presynaptic protein Brp, suggesting that Caz performs its physiological functions in neuronal cell bodies and/or their axons. In order to clarify whether or not disruption of the physiological functions of Caz are critical for the development of neurodegeneration even in the absence of abnormal Caz aggregates, we established fly models in which the *Caz* gene, which is the *Drosophila* FUS homologue, was knocked down. We demonstrated that neuron-specific knockdown of *Caz* did not affect the life span of the *Caz*-knockdown flies but did reduce the climbing abilities of adult flies, and also caused anatomical defects in presynaptic terminals of motoneurons in third instar larvae. These results suggested that a decrease in *Caz* expression is sufficient for the development of defects in locomotive abilities and for a decrease in the total length of synaptic branches of motoneurons at the NMJs in this *Drosophila* model. These data may indicate that the loss of physiological FUS functions in motoneurons would be more fundamental than the formation of cytoplasmic FUS aggregates in the pathogenesis of human FUS-related ALS/FTLD.

To eliminate the possibility that off-target effects of our RNAi construct that contained inverted repeats might generate the observed phenotypes, we used two different Caz inverted repeat constructs (*UAS-Caz-IR*$_{1\text{-}167}$ and *UAS-Caz-IR*$_{363\text{-}399}$) whose target sequences did not overlap with each other. We established four transgenic fly strains carrying *UAS-Caz-IR*$_{1\text{-}167}$ as listed in Table 1. We also obtained a fly strain carrying *UAS-Caz-IR*$_{363\text{-}399}$ from the Vienna *Drosophila* RNAi center (VDRC). This fly strain carries an RNAi that is targeted to the region corresponding to residues 363-399 of *Drosophila* Caz (*UAS-Caz-IR*$_{363\text{-}399}$), We then crossed these transgenic flies with the $elav^{3A}$-*GAL4* line to specifically express *Caz* double stranded RNA in neuronal tissues. Each independent fly strain carrying $elav^{3A}$/*Caz-IR*$_{1\text{-}167}$ showed essentially the same phenotype as the strain carrying *Caz-IR*$_{363\text{-}399}$/+;$elav^{3A}$/+. These results suggest that the phenotypes observed in the neuron-specific Caz-knockdown flies were not due to an off-target effect but rather to a reduction in Caz protein levels.

Mutations in the *FUS* gene are associated with inherited forms of both ALS and FTLD [15,16,18,19]. The *FUS* gene was originally identified in a study that found that the FUS protein forms part of a fusion protein with the transcription factor CHOP, which arises due to a chromosomal translocation in liposarcoma [26]. It has been reported that there are both dominantly and recessively inherited families of ALS with *FUS* mutations [15]. Before the discovery of these *FUS* mutations in familial ALS, mutations in the *TARDBP* gene that encodes another RNA-binding protein, TDP-43, had been reported to be associated with familial ALS and FTLD [7-14]. Both the *FUS* gene and the *TARDBP* gene encode an RNA-binding protein equipped with an RRM, and should therefore be involved in RNA processing, splicing, and RNA metabolism. Since FUS and TDP-43 have substantial similarities in their protein structure and putative functions, they could therefore cause ALS or FTLD through common pathogenic processes [2,38]. However, the mechanisms through which mutations in *FUS* or *TARDBP* cause ALS and FTLD are not known, and both toxic gain-of-function and loss-of-function models have been proposed [2,38]. ALS-associated mutant forms of TDP-43 and FUS are known to form abnormal cytosolic aggregates [15,16,35,39–41], and high-level overexpression of either wild-type or mutant TDP-43 is neurotoxic in mice, zebra fish and *Drosophila* [42–47]. One recent study reported that a *Drosophila* model in which targeted expression of mutant human FUS in *Drosophila* motor neurons led to locomotor dysfunction [48]. These findings would support the toxic gain-of-function model. However, overexpression of mutant proteins may also perturb the activity of endogenous TDP-43, supporting the loss-of-function model [49]. Similarly, the targeted expression model mentioned above reported that deletion of the nuclear export signal rescued toxicity associated with mutant FUS, suggesting that delocalization of FUS from the nucleus to the cytoplasm, namely the loss-of-nuclear-function, would be necessary for neurodegeneration [48]. In this study, we demonstrated that neuron-specific knockdown of *Caz*, the *Drosophila FUS* homologue, could induce a defect in fly locomotive abilities as well as degeneration of motoneurons at NMJs in the model flies. There has been one previous report that showed that flies lacking TBPH, the *Drosophila* TDP-43 homologue, present deficient locomotive behaviors, reduced life span and anatomical defects at the NMJs [37]. Regarding *FUS* and its homologues, one recent study reported that *Drosophila* mutants in which the *Caz* gene was disrupted exhibited

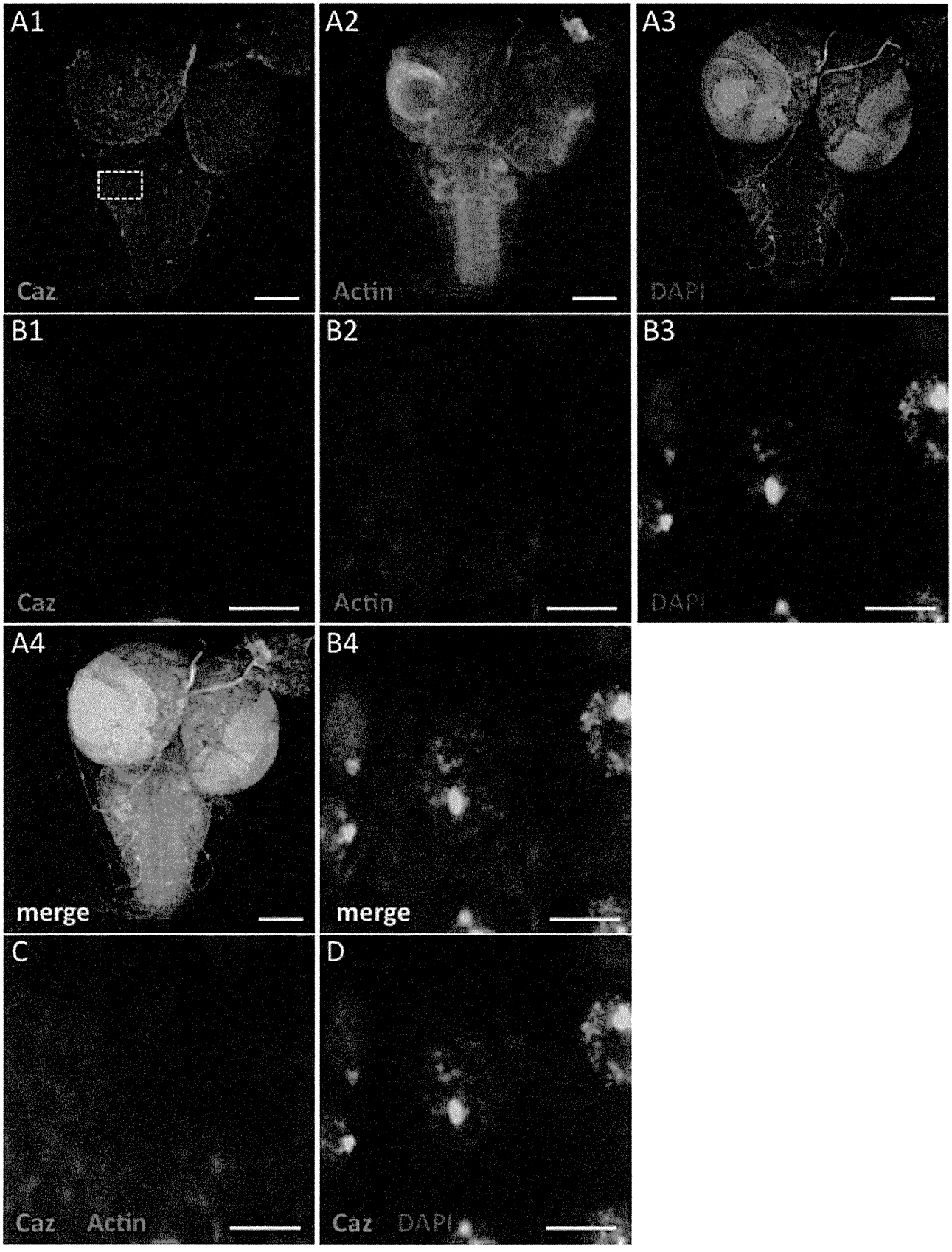

Figure 4. Intraneuronal localization of Caz in larval brains. Brain-ventral ganglia complexes from third instar larvae (A–D) were stained with the anti-Caz antibody (A-1, B-1), diamino-2-phenylidole (DAPI) (nuclear staining; A-2, B-2) or phalloidin (F-actin staining; A-3, B-3). Panels B-1 to B-4 are higher magnification images of the boxed area in A-1. Merged confocal images of A-1 to A-3, B-1 to B-3, B-1 and B-2, and B-1 and B-3 are shown in A-

4, B-4, C, and D, respectively. The bar indicates 100 μm (A) or 5 μm (B–D). Anti-Caz antibody-immunoreactivity was detected in the nucleus of neuronal cells and did not co-localize with actin filaments, which stained with phalloidin. Since Caz did not co-localize with DAPI, which stains chromosomes, Caz must therefore localize in the nucleoplasm.
doi:10.1371/journal.pone.0039483.g004

decreased adult viability, diminished locomotor speed and reduced life span compared with controls, and that these phenotypes were fully rescued by wild-type human *FUS*, but not by ALS-associated mutant *FUS* [50]. These reports, together with our results, demonstrated that a lack of physiological functions of FUS or TDP-43 in the nucleus is sufficient for induction of locomotive dysfunction and motoneuron degeneration, which recapitulate the phenotypes of ALS, and they therefore imply that the loss of physiological FUS functions are sufficient for the development of pathogenic processes similar to those that occur in FUS- or TDP-43-related ALS/FTLD, in the absence of cytosolic aggregates that may be toxic to motoneurons in ALS/FTLD.

There have been a few previous studies in which loss-of-function animal models of FUS-related human disorders were generated. FUS knockout mice show perinatal lethality and defects in B lymphocyte development [51]. Additionally, the hippocampal pyramidal neurons of these FUS-null mice exhibited abnormal spine morphology and lower spine density [52]. One report showed that surviving knockout mice exhibited male sterility [53]. However, the neurodegenerative phenotypes of these mice have not been reported to date. With regard to *Drosophila* models, one recent paper that was mentioned above presented a mutant fly strain (named the *Caz1* mutant) in which 58% of the *Caz* gene was deleted by creating a small genomic deletion [50]. This fly model developed a phenotype of disturbed locomotion that is similar to that observed in the *Caz*-knockdown flies in the present study. The differences between the *Caz1* mutant and our fly models were as follows; 1) the *Caz1* mutant did not show any morphological abnormalities at the NMJs i.e., shortening of the presynaptic terminals of motoneurons and decrease in the number of synaptic boutons, both of which were observed in our *Caz*-knockdown models. 2) The *Caz1* mutant showed reduced life spans, which were not observed in our models, and this life-span defect of *Caz1* mutant could be fully rescued by expression of wild-type fly *Caz* or wild-type human *FUS* in neurons using *elav-Gal4*. The difference in life span between the *Caz1* mutant and our *Caz*-knockdown models might be caused by differences in the expression pattern of the transgenes between the two models; in our fly models *Caz* gene expression was knocked down specifically in the nervous system, whereas, in the short-lived *Caz1* mutant flies, *Caz* was disrupted throughout the whole body. In our *Caz*-knockdown models, the expression of Caz protein was knocked down to 40–60% in the CNS (Figure 2), but their life spans were not reduced. Together with the fact that the reduced life span of the *Caz1* mutant was rescued by the neuronal expression of wild-type *Caz*, our results suggest that substantial expression of *Caz* in neuronal tissues, even though it is not fully expressed, could sufficiently keep their life spans within normal range. Our model flies also demonstrated that normal expression of *Caz* in neurons is essential for the elongation of synaptic branches of motoneurons at NMJs, and therefore that *Caz*-knockdown would induce impaired maturation of these synaptic branches, resulting in the observed locomotive deficit in our model flies, in the absence of any non-neuronal effect of the Caz protein.

In conclusion, we established fly models with neuron-specific knockdown of the *Drosophila* FUS homologue, and showed that those flies developed locomotive deficits as well as anatomical defects of motoneurons at NMJs. Our results indicate that the loss

Table 1. Established fly strains carrying *UAS-Caz-IR*.

Transgene	Strain	Chromosome linkage	Act5C-GAL4>		elav^{3A}-GAL4>
			28°C	25°C	
UAS-Caz-IR$_{1-167}$	3	III	lethal	lethal	LD (+)
	4	III	lethal	NE	ND
	11	II	lethal	NE	ND
	21	III	lethal	NE	ND
UAS-Caz-IR$_{180-346}$	11	II	NE	NE	NE
	12	II	NE	NE	NE
	17	II	NE	NE	ND
	22	III	NE	ND	LD (−)
	24	III	NE	NE	LD (−)
	32	III	ND	ND	ND
	33	III	ND	NE	ND
UAS-Caz-IR$_{363-399}$		II	NE	ND	LD (+)

LD: locomotive dysfunction, NE: no effect, ND: not determined.
doi:10.1371/journal.pone.0039483.t001

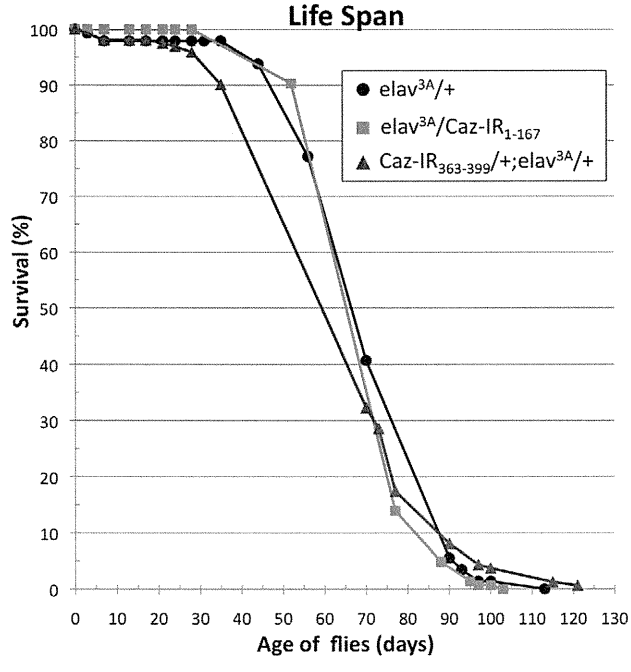

Figure 5. Life-span analyses of flies of each genotype. Percentage survival of adult male flies of the indicated genotypes is shown. Flies were collected from 20 different batches. The total number of flies counted was: *elav^{3A}/+* (n = 145), *elav^{3A}/Caz-IR$_{1-167}$* (n = 144) and *Caz-IR$_{363-399}$/+;elav^{3A}/+* (n = 161). There were no significant differences in the life span of flies with the indicated genotypes.
doi:10.1371/journal.pone.0039483.g005

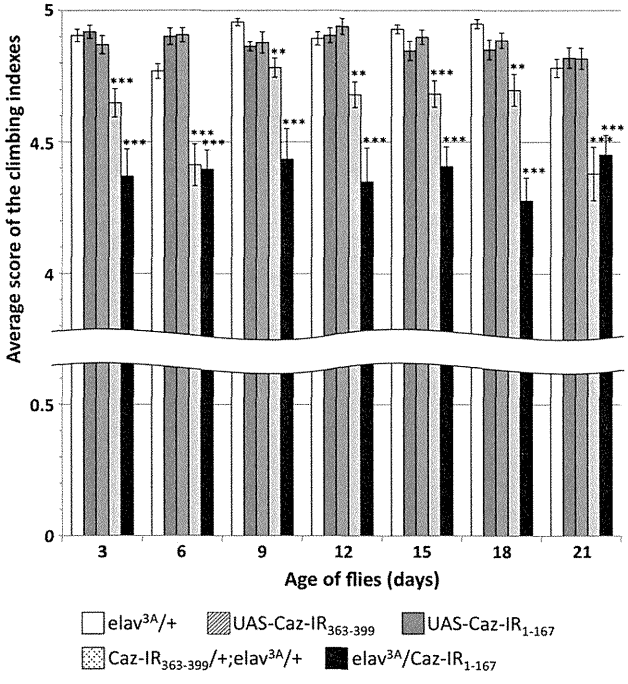

Figure 6. Climbing assays. Five independent tests were performed for each genotype. The total number of flies counted was: *elav^{3A}*/+ (a driver control, n = 309), *UAS-Caz-IR$_{363-399}$*/+ (a responder control, n = 222), *UAS-Caz-IR$_{1-167}$*/+ (a responder control, n = 246), *Caz-IR$_{363-399}$*/+;*elav^{3A}*/+ (n = 265) and *elav^{3A}*/*Caz-IR$_{1-167}$* (n = 238). There was no significant difference in climbing abilities between the driver and responder control flies in each day after eclosion. Flies carrying *elav^{3A}*/*Caz-IR$_{1-167}$* or *Caz-IR$_{363-399}$*/+;*elav^{3A}*/+ showed a significantly reduced ability to climb upwards compared to *elav^{3A}*/+ flies in each examined day. The horizontal bars indicate standard errors of mean values. ***p<0.001, **p<0.005.
doi:10.1371/journal.pone.0039483.g006

of physiological FUS functions in the nucleus is more likely to be the fundamental pathogenic mechanism that causes FUS-related ALS/FTLD than the toxicity of cytoplasmic aggregates. These data further indicate future research directions, suggesting that it will be necessary to identify target molecules, including nuclear proteins and/or RNA species that associate with FUS, in order to elucidate the molecular mechanisms leading to neuronal dysfunction in FUS-associated ALS/FTLD and to develop the disease-modifying therapies that are eagerly desired in those relentless neurodegenerative diseases. In any event, the *Drosophila* model that we established in the present study, which recapitulates key features of human ALS, would be suitable for the screening of genes and chemicals that can modify these pathogenic processes that lead to the degeneration of motoneurons in ALS.

Materials and Methods

Fly stocks

Fly stocks were maintained at 25°C on standard food containing 0.7% agar, 5% glucose and 7% dry yeast. Canton S was used as the wild type. W; *UAS-Caz-IR*; + (CG3606) was obtained from the Vienna *Drosophila* RNAi center (VDRC). The RNAi of this strain was targeted to the region corresponding to residues 363-399 of *Drosophila* Caz (*UAS-Caz-IR$_{363-399}$*). P{*GAL4-elav.L*}3A (elav^{3A}-GAL4) was provided by Dr. Bryan Stewart [54]. The Act5C-GAL4 strain was obtained from the Bloomington *Drosophila* stock center. Establishment of the lines carrying GMR-GAL4 was as described previously [55].

Comparison of amino acid sequences of human FUS and *Drosophila* Caz

The amino acid sequence of *Drosophila* Caz was retrieved from the Flybase (http://flybase.org). The identity and the similarity of *Drosophila* Caz and human FUS were compared using BLAST (http://blast.genome.jp/) and FASTA (http://fasta.genome.jp/). FASTA was used for comparison of the entire sequences, and BLAST was used for comparison of each corresponding domain between Caz and FUS.

Establishment of the transgenic flies

To establish transgenic fly lines carrying *UAS-Caz-IR*, 500-bp fragments of Caz ORFs (*UAS-Caz-IR$_{1-167}$*; 5′-ATGGAACGTGGCGGTTATGGTGGT to 5′-AGAACAAGGAGACCGGCGC, *UAS-Caz-IR$_{180-346}$*; 5′-ATGCTGCACAATCCGCCATTGAAT to 5′-CAACAGAGATCGCGGTGGC) from *Caz* cDNA clone CG3606 were amplified, and then individually cloned into the pENTR/D-TOPO vector (Invitrogen Life Technologies Japan Corporation, Tokyo, Japan), in which each trigger sequence of *Caz* was placed between the *attL1* and *attL2* recombination sequences. Following confirmation by sequencing, two copies of each trigger sequence were transferred into the pRISE transformation vector that contains a characteristic inverted repeat of *attR1-cm^r-ccdB-attR2* in a recombination cassette by an *in vitro* reaction mediated by LR Clonase (Invitrogen), a DNA recombinase that specifically recognizes the *attL* and *attR2* target sites [56]. Due to the recombination reaction between the *attL* and *attR2* sites, the ccdB sequence was replaced by the target cDNA, resulting in the cloning of a head-to-head inverted repeat (IR) of Caz into the plasmid.

These plasmids were verified by sequencing and then injected into embryos to obtain stable transformant lines carrying *UAS-Caz-IR*. P element-mediated germ line transformation was carried out as described previously [57], and F1 transformants were selected on the basis of white-eye color rescue [58]. Four and seven transgenic strains carrying *UAS-Caz-IR$_{1-167}$* and *UAS-Caz-IR$_{180-346}$* were established, respectively (responder controls), as listed in Table 1. To drive expression of *Caz* double stranded RNA in the whole body of the flies or specifically in neuronal tissues, we crossed the transgenic flies with either the *Act5C-GAL4* line or the *elav^{3A}-GAL4* line (*elav^{3A}-GAL4*/+; a driver control). Each transgenic strain showed a consistent phenotype (Table 1).

Production of rabbit anti-Caz antibodies

Rabbit anti-Caz antibodies were produced by MEDICAL & BIOLOGICAL LABORATORIES Co., Ltd (MBL, Ina, Japan). The peptides, N-NKTGNYEPPPNYGKQGC-C (residues 29–45; the underlined C residue C was an added residue) and N-CRDGGPMRNDGGMRSRPY-C (residues 383–399), which correspond respectively to the N- and C-terminal sequences of Caz, were individually conjugated with KLH (Keyhole limpet hemocyanin). These two KLH-conjugated peptides were mixed with Freund's complete adjuvant to provide a suspension, which was injected intradermally into rabbits (Female Japanese White). The rabbits were then boosted with inoculations of an immunogen of the same quality once a week for 7 weeks, and a terminal bleed was performed to collect the maximum amount of serum. The serum was purified by affinity chromatography against the synthesized peptides using a Protein G column.

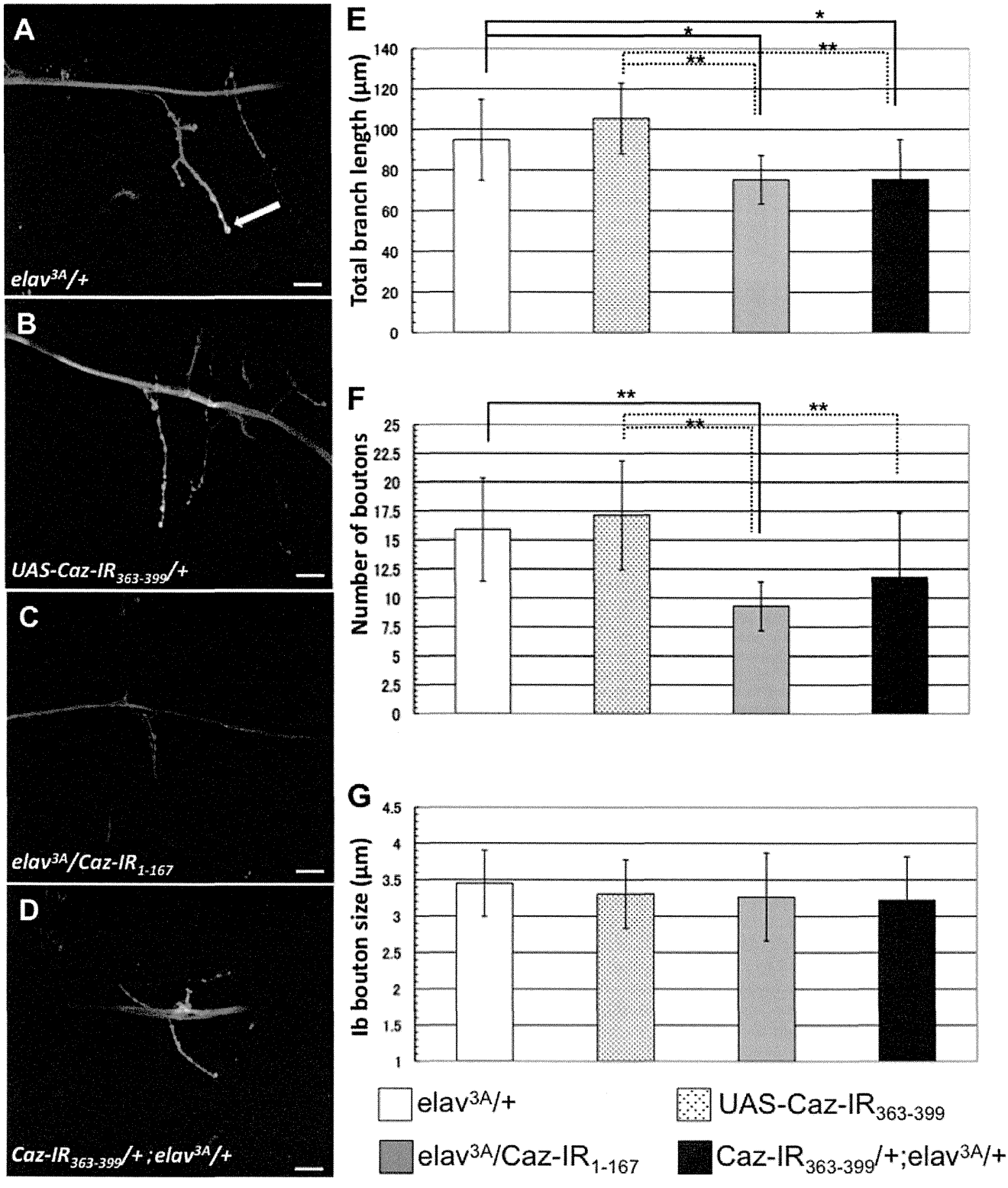

Figure 7. Confocal images of anti-HRP staining of muscle 4 synapses in third instar larvae. A representative image of the indicated genotypes is shown; (A) *elav*^{3A}/+ (a driver control), (B) *UAS-Caz-IR*$_{363\text{-}399}$/+ (a responder control), (C) *elav*^{3A}/*Caz-IR*$_{1\text{-}167}$ and (D) *Caz-IR*$_{363\text{-}399}$/+;*elav*^{3A}/+. The bar indicates 20 μm. (E) Total branch length of the NMJ from muscle 4 for each of the indicated genotypes. n = 9 for each genotype. (F, G) The number (F) and the size (G) of the synaptic boutons for each of the indicated genotypes. (F) n = 9 for each genotype. (G) The size of Ib bouton (indicated with an arrow in A) was measured. n = 30 for *elav*^{3A}/+, n = 34 for *Caz-IR*$_{363\text{-}399}$/+, n = 27 for *elav*^{3A}/*Caz-IR*$_{1\text{-}167}$, n = 34 for *Caz-IR*$_{363\text{-}399}$/+*elav*^{3A}/+. The *Caz*-knockdown flies did not show any apparent changes in NMJ structure. However, the total length of synaptic branches of the motoneurons was significantly decreased in each Caz-knockdown fly strain (*elav*^{3A}/*Caz-IR*$_{1\text{-}167}$ and *Caz-IR*$_{363\text{-}399}$/+;*elav*^{3A}/+) compared to the both driver and responder control flies (E). The flies carrying *elav*^{3A}/*Caz-IR*$_{1\text{-}167}$ showed the significantly decreased number of the synaptic boutons compared to the

both driver and responder control flies, and so did the flies carrying *Caz-IR*$_{363\text{-}399}$/+;*elav*^{3A}/+ compared to the responder controls (F). There were no significant differences in the size of synaptic boutons among those 4 genotypes (G). The horizontal bars indicate standard errors of mean values. *p<0.05, **p<0.01.
doi:10.1371/journal.pone.0039483.g007

Immunoblotting analysis

Protein extracts from the central nervous system (CNS) of *Drosophila* carrying *elav*^{3A}*-GAL4/+*, *UAS-Caz-IR*$_{180\text{-}346}$/+, *UAS-Caz-IR*$_{1\text{-}167}$/+ and *elav*^{3A}*-GAL4>UAS-Caz-IR* were prepared as previously described [59]. Briefly, the CNS was excised from third instar larvae and homogenized in a sample buffer containing 50 mM Tris-HCl (pH 6.8), 2% SDS, 10% glycerol, 0.1% bromophenol blue and 1.2% β-mercaptoethanol. The homogenates were boiled at 100°C for 5 min, and then centrifuged. The supernatants (extracts) were electrophoretically separated on SDS-polyacrylamide gels containing 12% acrylamide and then transferred to polyvinylidene difluoride (PVDF) membranes (Bio-Rad, Osaka, Japan). The blotted membranes were blocked with TBS/0.05% Tween containing 5% skim milk for 1 h at 25°C, followed by incubation with rabbit polyclonal anti-Caz at a 1:5,000 dilution for 16 h at 4°C. After washing, the membranes were incubated with HRP-conjugated anti-rabbit IgG (GE Healthcare Bioscience, Tokyo, Japan) at 1:10,000 dilution for 2 h at 25°C. Antibody binding was detected using ECL Western blotting detection reagents (GE Healthcare Bioscience) and images were analyzed using a Lumivision Pro HSII image analyzer (Aisin Seiki, Kariya, Japan). To ensure equal protein loading in each lane, the membranes were also probed with an anti-α-tubulin antibody after stripping the complex of anti-Caz antibody and HRP-conjugated anti-rabbit IgG. For the detection of α-tubulin, mouse anti-α-tubulin monoclonal antibody (1:5,000 dilution, Sigma, Tokyo, Japan) and an HRP-conjugated anti-mouse IgG (1:10,000 dilution, GE Healthcare Bioscience) were used as the primary and secondary antibodies, respectively.

Immunostaining

For immunohistochemical analysis, CNS tissues of third instar larvae and adult flies were dissected, and fixed in 4% paraformaldehyde/PBS for 15 min at 25°C. After washing with PBS containing 0.3% Triton X-100, the samples were blocked with blocking buffer (PBS containing 0.15% Triton X-100 and 10% normal goat serum) for 30 min at 25°C, and then incubated with diluted primary antibodies in the blocking buffer for 20 h at 4°C. The following antibodies were used; 1:1,000 diluted rabbit anti-Caz antibody and 1:100 diluted mouse anti-Brp antibody (Developmental Studies Hybridoma Bank [DSBH] nc82). After extensive washing with PBS containing 0.3% Triton X-100, samples were incubated with secondary antibodies labeled with either Alexa 546 or Alexa 488 (1:400; Invitrogen) diluted in the blocking buffer, in the dark, for 2 h at 25°C. After extensive washing with PBS containing 0.3% Triton X-100 and PBS, samples were mounted in Fluoroguard Antifade Reagent (Bio-Rad) and observed under a Zeiss LSM510 confocal laser scanning microscope.

For NMJ staining, third instar larvae were dissected in HL3 saline [60] and fixed in 4% paraformaldehyde/PBS for 30 min. The blocking buffer was 2% bovine serum albumin (BSA)/PBS/0.1% TritonX-100. FITC-conjugated goat anti-HRP (1:1,000, MP Biochemicals) was used as the detection antibody. The samples were mounted and observed under a Zeiss LSM510 confocal laser scanning microscope. MN4 (Ib) in muscle 4 in abdominal segment 2 was quantified. Images were acquired using a Zeiss LSM510 by merging 1 μm interval z-sections onto a single plane. Nerve terminal branch lengths were measured using Image J software.

To determine whether Caz is present in the nucleus or not, CNS tissues of third instar larvae were dissected, and fixed in 4% paraformaldehyde/PBS for 15 min at 25°C. After washing with PBS containing 0.3% Triton X-100, the samples were incubated with Alexa 488-conjugated phalloidin (1 unit/200 μl) in PBS containing 0.3% Triton X-100 for 20 min at 25°C. The samples were then blocked and reacted with the primary and the secondary antibodies as described for the immunohistochemical analysis described above, except that the mouse anti-Brp antibody was not used. After extensive washing with PBS containing 0.3% Triton X-100, the samples were stained with DAPI (0.5 μg/ml)/PBS/0.1% Triton X-100. Following washing with PBS containing 0.1% Triton X-100 and PBS, the samples were mounted and observed under a confocal laser scanning microscope (OLYMPUS Fluoview FV10i).

Longevity assay

Longevity assays were carried out in a humidified, temperature controlled incubator at 25°C and 60% humidity on a 12-h light and 12-h dark cycle on standard fly food. Flies carrying *elav*^{3A}*-GAL4/+* and *elav*^{3A}*-GAL4>UAS-Caz-IR* were placed at 28°C, and newly eclosed adult flies were separated and placed in vials at a low density (10–20 flies per vial) with a male: female ratio of 1: 1. Every 3 days, they were transferred to new tubes containing fresh food and deaths were scored. Survival rate was determined by plotting a graph of the percentage of surviving flies versus days.

Climbing assay

Climbing assays were performed as described previously [61]. Flies carrying *elav*^{3A}*-GAL4/+*, *UAS-Caz-IR*$_{363\text{-}399}$/+, *UAS-Caz-IR*$_{1\text{-}167}$/+, and *elav*^{3A}*-GAL4>UAS-Caz-IR* were placed at 28°C, and newly eclosed adult flies were separated and placed in vials at a density of 30 flies per vial (15 males and 15 females). Flies were transferred, without anesthesia, to a conical tube. The tube was tapped to collect the flies to the bottom, and they were then given 30 s to climb the wall. After 30 s the flies were collected at the bottom by tapping of the tube, and were again allowed to climb for 30 s. Similar procedures, all of which were videotaped, were repeated five times in total. For all of the climbing experiments, the height to which each fly climbed was scored as follows (score (height climbed)); 0 (less than 2 cm), 1 (between 2 and 3.9 cm), 2 (between 4 and 5.9 cm), 3 (between 6 and 7.9 cm), 4 (between 8 and 9.9 cm) and 5 (greater than 10 cm). The climbing index of each fly strain was calculated as follows; the sum of the products of each score multiplied by the number of flies for which that score was recorded, was calculated, and this number was then divided by five times the total number of flies examined. These climbing assays were carried out every 3 days until the 18th day after eclosion.

Data analysis

All statistical analyses were performed using Microsoft Excel. The Mann-Whitney test was used for assessment of the statistical significance of comparisons between groups of data concerning median life span. For other assays the two-way ANOVA was used to determine the statistical significance of comparisons between groups of data. When the two-way ANOVA showed significant

variation among the groups, Dunnet's test was subsequently used for pairwise comparisons of groups. All data are shown as means ± SEM.

Author Contributions

Conceived and designed the experiments: TT MY MN TY TM. Performed the experiments: HS MS YA MY. Analyzed the data: TT HS MS MY. Contributed reagents/materials/analysis tools: NF YN MN. Wrote the paper: TT MS HS MY.

References

1. Boillée S, Vande Velde C, Cleveland DW (2006) ALS: a disease of motor neurons and their nonneuronal neighbors. Neuron 52: 39–59.
2. Mackenzie IR, Rademakers R, Neumann M (2010) TDP-43 and FUS in amyotrophic lateral sclerosis and frontotemporal dementia. Lancet Neurol 9: 995–1007.
3. Lomen-Hoerth C, Anderson T, Miller B (2002) The overlap of amyotrophic lateral sclerosis and frontotemporal dementia. Neurology 59: 1077–1079.
4. Murphy JM, Henry RG, Langmore S, Kramer JH, Miller BL, et al. (2007) Continuum of frontal lobe impairment in amyotrophic lateral sclerosis. Arch Neurol 64: 530–534.
5. Neumann M, Sampathu DM, Kwong LK, Truax AC, Micsenyi MC, et al. (2006) Ubiquitinated TDP-43 in frontotemporal lobar degeneration and amyotrophic lateral sclerosis. Science 314: 130–133.
6. Arai T, Hasegawa M, Akiyama H, Ikeda K, Nonaka T, et al. (2006) TDP-43 is a component of ubiquitin-positive tau-negative inclusions in frontotemporal lobar degeneration and amyotrophic lateral sclerosis. Biochem Biophys Res Commun 351: 602–611.
7. Gitcho MA, Baloh RH, Chakraverty S, Mayo K, Norton JB, et al. (2008) TDP-43 A315T mutation in familial motor neuron disease. Ann Neurol 63: 535–538.
8. Yokoseki A, Shiga A, Tan CF, Tagawa A, Kaneko H, et al. (2008) TDP-43 mutation in familial amyotrophic lateral sclerosis. Ann Neurol 63: 538–542.
9. Lacomblez L, Pochigaeva K, Salachas F, Pradat PF, Camu W, et al. (2008) TARDBP mutations in individuals with sporadic and familial amyotrophic lateral sclerosis. Nat Genet 40: 572–574.
10. Sreedharan J, Blair IP, Tripathi VB, Hu X, Vance C, et al. (2008) TDP-43 mutations in familial and sporadic amyotrophic lateral sclerosis. Science 319: 1668–1672.
11. Van Deerlin VM, Leverenz JB, Bekris LM, Bird TD, Yuan W, et al. (2008) TARDBP mutations in amyotrophic lateral sclerosis with TDP-43 neuropathology: a genetic and histopathological analysis. Lancet Neurol 7: 409–416.
12. Pesiridis GS, Lee VM, Trojanowski JQ (2009) Mutations in TDP-43 link glycine-rich domain functions to amyotrophic lateral sclerosis. Hum Mol Genet 18: R156–R162.
13. Benajiba L, Le Ber I, Camuzat A, Lacoste M, Thomas-Anterion C, et al. (2009) TARDBP mutations in motoneuron disease with frontotemporal lobar degeneration. Ann Neurol 65: 470–473.
14. Kovacs GG, Murrell JR, Horvath S, Haraszti L, Majtenyi K, et al. (2009) TARDBP variation associated with frontotemporal dementia, supranuclear gaze palsy, and chorea. Mov Disord 24: 1843–1847.
15. Kwiatkowski TJ Jr, Bosco DA, Leclerc AL, Tamrazian E, Vanderburg CR, et al. (2009) Mutations in the FUS/TLS gene on chromosome 16 cause familial amyotrophic lateral sclerosis. Science 323: 1205–1208.
16. Vance C, Rogelj B, Hortobágyi T, De Vos KJ, Nishimura AL, et al. (2009) Mutations in FUS, an RNA processing protein, cause familial amyotrophic lateral sclerosis type 6. Science 323: 1208–1211.
17. Hewitt C, Kirby J, Highley JR, Hartley JA, Hibberd R, et al. (2010) Novel FUS/TLS mutations and pathology in familial and sporadic amyotrophic lateral sclerosis. Arch Neurol 67: 455–461.
18. Broustal O, Camuzat A, Guillot-Noël L, Guy N, Millecamps S, et al. (2010) FUS mutations in frontotemporal lobar degeneration with amyotrophic lateral sclerosis. J Alzheimers Dis 22: 765–769.
19. Mackenzie IR, Rademakers R, Neumann M (2010) TDP-43 and FUS in amyotrophic lateral sclerosis and frontotemporal dementia. Lancet Neurol 9: 995–1007.
20. Munoz DG, Neumann M, Kusaka H, Yokota O, Ishihara K, et al. (2009) FUS pathology in basophilic inclusion body disease. Acta Neuropathol 118: 617–627.
21. Huang EJ, Zhang J, Geser F, Trojanowski JQ, Strober JB, et al. (2010) Extensive FUS-immunoreactive pathology in juvenile amyotrophic lateral sclerosis with basophilic inclusions. Brain Pathol 20: 1069–1076.
22. Urwin H, Josephs KA, Rohrer JD, Mackenzie IR, Neumann M, et al. (2010) FUS pathology defines the majority of tau- and TDP-43-negative frontotemporal lobar degeneration. Acta Neuropathol 120: 33–41.
23. Lagier-Tourenne C, Cleveland DW (2009) Rethinking ALS: the FUS about TDP-43. Cell 136: 1001–1004.
24. Doi H, Koyano S, Suzuki Y, Nukina N, Kuroiwa Y (2010) The RNA-binding protein FUS/TLS is a common aggregate-interacting protein in polyglutamine diseases. Neurosci Res 66: 131–133.
25. Woulfe J, Gray DA, Mackenzie IR (2010) FUS-immunoreactive intranuclear inclusions in neurodegenerative disease. Brain Pathol 20: 589–597
26. Crozat A, Aman P, Mandahl N, Ron D (1993) Fusion of CHOP to a novel RNA-binding protein in human myxoid liposarcoma. Nature 363: 640–644.
27. Zinszner H, Sok J, Immanuel D, Yin Y, Ron D (1997) TLS (FUS) binds RNA in vivo and engages in nucleo-cytoplasmic shuttling. J Cell Sci 110: 1741–1750.
28. Kasyapa CS, Kunapuli P, Cowell JK (2005) Mass spectroscopy identifies the splicing-associated proteins, PSF, hnRNP H3, hnRNP A2/B1, and TLS/FUS as interacting partners of the ZNF198 protein associated with rearrangement in myeloproliferative disease. Exp Cell Res 309: 78–85.
29. Andersson MK, Ståhlberg A, Arvidsson Y, Olofsson A, Semb H, et al. (2008) The multifunctional FUS, EWS and TAF15 proto-oncoproteins show cell type-specific expression patterns and involvement in cell spreading and stress response. BMC Cell Biol 9: 37–54.
30. Fujii R, Okabe S, Urushido T, Inoue K, Yoshimura A, et al. (2005) The RNA binding protein TLS is translocated to dendritic spines by mGluR5 activation and regulates spine morphology. Curr Biol 15: 587–593.
31. Lee BJ, Cansizoglu AE, Süel KE, Louis TH, Zhang Z, et al. (2006) Rules for nuclear localization sequence recognition by karyopherin beta 2. Cell 126: 543–558.
32. Dormann D, Rodde R, Edbauer D, Bentmann E, Fischer I, et al. (2010) ALS-associated fused in sarcoma (FUS) mutations disrupt Transportin-mediated nuclear import. EMBO J 29: 2841–2857.
33. Ito D, Seki M, Tsunoda Y, Uchiyama H, Suzuki N (2011) Nuclear transport impairment of amyotrophic lateral sclerosis-linked mutations in FUS/TLS. Ann Neurol 69: 152–162.
34. Kino Y, Washizu C, Aquilanti E, Okuno M, Kurosawa M, et al. (2011) Intracellular localization and splicing regulation of FUS/TLS are variably affected by amyotrophic lateral sclerosis-linked mutations. Nucleic Acids Res 39: 2781–2798.
35. Bosco DA, Lemay N, Ko HK, Zhou H, Burke C, et al. (2010) Mutant FUS proteins that cause amyotrophic lateral sclerosis incorporate into stress granules. Hum Mol Genet 19: 4160–4175.
36. Stolow DT, Haynes SR (1995) Cabeza, a *Drosophila* gene encoding a novel RNA binding protein, shares homology with EWS and TLS, two genes involved in human sarcoma formation. Nucleic Acids Res 23: 835–843.
37. Feiguin F, Godena VK, Romano G, D'Ambrogio A, Klima R, et al. (2009) Depletion of TDP-43 affects Drosophila motoneurons terminal synapsis and locomotive behavior. FEBS Lett 583: 1586–1592.
38. Lagier-Tourenne C, Polymenidou M, Cleveland DW (2010) TDP-43 and FUS/TLS: emerging roles in RNA processing and neurodegeneration. Hum Mol Genet 19: R46–R64.
39. DeJesus-Hernandez M, Kocerha J, Finch N, Crook R, Baker M, et al. (2010) De novo truncating FUS gene mutation as a cause of sporadic amyotrophic lateral sclerosis. Hum Mutat 31: E1377–E1389.
40. Sun Z, Diaz Z, Fang X, Hart MP, Chesi A, et al. (2011) Molecular determinants and genetic modifiers of aggregation and toxicity for the ALS disease protein FUS/TLS. PLoS Biol 9: e1000614.
41. Buratti E, Baralle FE (2009) The molecular links between TDP-43 dysfunction and neurodegeneration. Adv Genet 66: 1–34.
42. Wegorzewska I, Bell S, Cairns NJ, Miller TM, Baloh RH (2009) TDP-43 mutant transgenic mice develop features of ALS and frontotemporal lobar degeneration. Proc Natl Acad Sci U S A 106: 18809–18814.
43. Kabashi E, Lin L, Tradewell ML, Dion PA, Bercier V, et al. (2010) Gain and loss of function of ALS-related mutations of TARDBP (TDP-43) cause motor deficits in vivo. Hum Mol Genet 19: 671–683.
44. Li Y, Ray P, Rao EJ, Shi C, Guo W, et al. (2010) A *Drosophila* model for TDP-43 proteinopathy. Proc Natl Acad Sci U S A 107: 3169–3174.
45. Wils H, Kleinberger G, Janssens J, Pereson S, Joris G, et al. (2010) TDP-43 transgenic mice develop spastic paralysis and neuronal inclusions characteristic of ALS and frontotemporal lobar degeneration. Proc Natl Acad Sci U S A 107: 3858–3863.
46. Hanson KA, Kim SH, Wassarman DA, Tibbetts RS (2010) Ubiquilin modifies TDP-43 toxicity in a *Drosophila* model of amyotrophic lateral sclerosis (ALS). J Biol Chem 285: 11068–11072.
47. Miguel L, Frébourg T, Campion D, Lecourtois M (2011) Both cytoplasmic and nuclear accumulations of the protein are neurotoxic in *Drosophila* models of TDP-43 proteinopathies. Neurobiol Dis 41: 398–406.
48. Lanson NA Jr, Maltare A, King H, Smith R, Kim JH, et al. (2011) A *Drosophila* model of FUS-related neurodegeneration reveals genetic interaction between FUS and TDP-43. Hum Mol Genet 20: 2510–2523.
49. Igaz LM, Kwong LK, Lee EB, Chen-Plotkin A, Swanson E, et al. (2011) Dysregulation of the ALS-associated gene TDP-43 leads to neuronal death and degeneration in mice. J Clin Invest 121: 726–738.
50. Wang JW, Brent JR, Tomlinson A, Shneider NA, McCabe BD (2011) The ALS-associated proteins FUS and TDP-43 function together to affect Drosophila locomotion and life span. J Clin Invest 121: 4118–4126.
51. Hicks GG, Singh N, Nashabi A, Mai S, Bozek G, et al. (2000) Fus deficiency in mice results in defective B-lymphocyte development and activation, high levels of chromosomal instability and perinatal death. Nat Genet 24: 175–179.

52. Fujii R, Okabe S, Urushido T, Inoue K, Yoshimura A, et al. (2005) The RNA binding protein TLS is translocated to dendritic spines by mGluR5 activation and regulates spine morphology. Curr Biol 15: 587–593.
53. Kuroda M, Sok J, Webb L, Baechtold H, Urano F, et al. (2000) Male sterility and enhanced radiation sensitivity in TLS(-/-) mice. EMBO J 19: 453–462.
54. Stewart BA, Mohtashami M, Rivlin P, Deitcher DL, Trimble WS, et al. (2002) Dominant-negative NSF2 disrupts the structure and function of *Drosophila* neuromuscular synapses. J Neurobiol 51: 261–271.
55. Takahashi Y, Hirose F, Matsukage A, Yamaguchi M (1999) Identification of three conserved regions in the DREF transcription factors from *Drosophila melanogaster* and *Drosophila virilis*. Nucleic Acids Res 27: 510–516.
56. Kondo T, Inagaki S, Yasuda K, Kageyama Y (2006) Rapid construction of *Drosophila* RNAi transgenes using pRISE, a P-element-mediated transformation vector exploiting an in vitro recombination system. Genes Genet Syst 81: 129–134.
57. Spradling AC (1986) P-element-mediated transformation. In: Roberts DB, editor, *Drosophila*: a practical approach. Oxford: IRL Press.
58. Robertson HM, Preston CR, Phillis RW, Johnson-Schlitz DM, Benz WK, et al. (1988) A stable genomic source of P element transposase in *Drosophila melanogaster*. Genetics 118: 461–470.
59. Nagai R, Hashimoto R, Tanaka Y, Taguchi O, Sato M, et al. (2010) Syntrophin-2 is required for eye development in *Drosophila*. Exp Cell Res 316: 272–285.
60. Stewart BA, Atwood HL, Renger JJ, Wang J, Wu CF (1994) Improved stability of *Drosophila* larval neuromuscular preparations in haemolymph-like physiological solutions. J Comp Physiol A 175: 179–191.
61. Shcherbata HR, Yatsenko AS, Patterson L, Sood VD, Nudel U, et al. (2007) Dissecting muscle and neuronal disorders in a Drosophila model of muscular dystrophy. EMBO J 26: 481–493.
62. Prasad DD, Ouchida M, Lee L, Rao VN, Reddy ES (1994) TLS/FUS fusion domain of TLS/FUS-erg chimeric protein resulting from the t(16;21) chromosomal translocation in human myeloid leukemia functions as a transcriptional activation domain. Oncogene 9: 3717–3729.
63. Cushman M, Johnson BS, King OD, Gitler AD, Shorter J (2010) Prion-like disorders: blurring the divide between transmissibility and infectivity. J Cell Sci 123: 1191–1201.
64. Udan M, Baloh RH (2011) Implications of the prion-related Q/N domains in TDP-43 and FUS. Prion 5: 1–5.
65. Lerga A, Hallier M, Delva L, Orvain C, Gallais I, et al. (2001) Identification of an RNA binding specificity for the potential splicing factor TLS. J Biol Chem 276: 6807–6816.
66. Iko Y, Kodama TS, Kasai N, Oyama T, Morita EH, et al. (2004) Domain architectures and characterization of an RNA-binding protein, TLS. J Biol Chem 279: 44834–44840.

Neurotherapeutics
DOI 10.1007/s13311-013-0184-7

Inhibition of Protein Misfolding/Aggregation Using Polyglutamine Binding Peptide QBP1 as a Therapy for the Polyglutamine Diseases

H. Akiko Popiel · Toshihide Takeuchi · James R. Burke · Warren J. Strittmatter · Tatsushi Toda · Keiji Wada · Yoshitaka Nagai

Abstract Protein misfolding and aggregation in the brain have been recognized to be crucial in the pathogenesis of various neurodegenerative diseases, including Alzheimer's, Parkinson's, and the polyglutamine (polyQ) diseases, which are collectively called the "protein misfolding diseases". In the polyQ diseases, an abnormally expanded polyQ stretch in the responsible proteins causes the proteins to misfold and aggregate, eventually resulting in neurodegeneration. Hypothesizing that polyQ protein misfolding and aggregation could be inhibited by molecules specifically binding to the expanded polyQ stretch, we identified polyQ binding peptide 1 (QBP1). We show that QBP1 does, indeed, inhibit misfolding and aggregation of the expanded polyQ protein *in vitro*. Furthermore overexpression of QBP1 by the crossing of transgenic animals inhibits neurodegeneration in *Drosophila* models of the polyQ diseases. We also introduce our attempts to deliver QBP1 into the brain by administration using viral vectors and protein transduction domains. Interestingly, recent data suggest that QBP1 can also inhibit the misfolding/aggregation of proteins responsible for other protein misfolding diseases, highlighting the potential of QBP1 as a general therapeutic molecule for a wide range of neurodegenerative diseases. We hope that in the near future, aggregation inhibitor-based drugs will be developed and bring relief to patients suffering from these currently intractable protein misfolding diseases.

Keywords Polyglutamine disease · Neurodegeneration · QBP1 · Protein aggregation · Inhibitor peptide · Therapy

H. A. Popiel · T. Takeuchi · K. Wada · Y. Nagai (✉)
Department of Degenerative Neurological Diseases, National Institute of Neuroscience, National Center of Neurology and Psychiatry, 4-1-1 Ogawa Higashi,
Kodaira, Tokyo 187-8502, Japan
e-mail: nagai@ncnp.go.jp

J. R. Burke · W. J. Strittmatter
Department of Medicine (Neurology) and Deane Laboratory, Duke University Medical Center, Durham, NC 27710, USA

T. Toda
Division of Neurology/Molecular Brain Science, Kobe University Graduate School of Medicine, Kobe 650-0017, Japan

Y. Nagai
Core Research for Evolutional Science and Technology (CREST), Japan Science and Technology Agency, Saitama 332-0012, Japan

Published online: 16 March 2013

Introduction

Recent accumulating evidence has indicated that many neurodegenerative diseases including Alzheimer's disease (AD), Parkinson's disease (PD), the polyglutamine (polyQ) diseases, amyotrophic lateral sclerosis (ALS), and the prion diseases share a common pathomechanism involving protein misfolding/aggregation and their accumulation in the brain. Pathologic and biochemical studies have revealed that various protein depositions are found inside and outside of neurons in the diseased brains, such as senile plaques composed of amyloid-β in AD [1] and Lewy bodies composed of α-synuclein in PD [2]. Although the significance of these protein depositions on disease pathology long remained controversial, recent molecular genetics studies revealed that the mutations responsible for the inherited forms of these neurodegenerative diseases render the proteins to be prone to misfolding and aggregating, or lead to the overproduction of aggregation-prone proteins [3–5]. Furthermore, not only the inherited forms of these diseases, but the sporadic cases also exhibit similar protein accumulations in the brain, further indicating that misfolding and abnormal aggregation of proteins are crucial in the pathogenesis of these

neurodegenerative diseases, which are, hence, collectively called the "protein misfolding diseases" [3–5].

In this review we will introduce our research towards establishing a therapy for the polyQ diseases by targeting protein misfolding and aggregation using polyglutamine binding peptide 1 (QBP1).

The Polyglutamine Diseases

The polyQ diseases are a group of neurodegenerative diseases caused by a common genetic mutation, namely an expansion (>40) of the CAG repeat encoding a polyQ stretch in each unrelated disease-causing gene [6, 7]. Nine diseases currently belong to this group, including Huntington's disease, spinocerebellar ataxia type 1, 2, 3, 6, 7, and 17, dentatorubral pallidoluysian atrophy, and spinobulbar muscular atrophy (SBMA) [7]. In these diseases, progressive degeneration of neurons in brain areas specific for each disease occurs, causing various neurologic and psychiatric symptoms corresponding to each affected brain area.

Numerous sources of evidence has led to the consensus that the expanded polyQ stretch itself is the cause of the polyQ diseases based on a gain of toxic function mechanism. First, they are inherited in an autosomal dominant manner (except for SBMA). Second, the polyQ stretch is the only homologous sequence among the disease-causing proteins, which show no other functional or sequence similarity. Furthermore, the polyQ stretch is the major determinant of disease, as shown by a threshold between normal and disease of 35–40 repeats (except for spinocerebellar ataxia type 6), and a tight correlation between polyQ repeat length and the age of disease onset and severity. Third, loss-of-function mutations in the disease-causing gene of SBMA (androgen receptor gene) do not cause neurodegenerative disease. Finally, expression of an expanded polyQ stretch alone or even inserted into an unrelated protein is sufficient to cause neurodegeneration in various experimental animal models [8–11].

To study the molecular pathomechanisms of, and potential therapies for, the protein misfolding diseases, the polyQ diseases are the most suitable model as they possess the following characteristics. First, as they are determined almost solely by a monogenic mutation, it is relatively easy to establish genetic models, unlike the other diseases, which are caused by multiple genetic and environmental factors. Second, as there is a strong genotype–phenotype correlation, the severity of the experimental model can be manipulated as suitable for analysis. Our group has therefore been using the polyQ diseases as a model of the protein misfolding diseases, towards establishing a therapy for these diseases.

In the common molecular pathogenesis of the polyQ diseases, proteins with an expanded polyQ stretch become misfolded and undergo a toxic conformational transition to a β-sheet dominant monomer [12], then form oligomers/aggregates, and, subsequently, accumulate as inclusion bodies within neurons, eventually resulting in neurodegeneration [13–17]. Although therapeutic strategies against various cellular processes thought to be eventually impaired in the polyQ diseases have been investigated [16, 18], they have resulted in limited therapeutic effects, as numerous processes are affected by the expanded polyQ protein [19]. In contrast to the downstream effects, misfolding and aggregation of the expanded polyQ protein are ideal therapeutic targets as they are the most initial pathogenic events, and therefore their inhibition is expected to result in the suppression of a broad range of downstream pathogenic events [14, 15, 20–22] (Fig. 1). We therefore aimed to establish a therapy targeting misfolding and aggregation of the expanded polyQ protein.

Identification of QBP1

We hypothesized that misfolding/aggregation of the expanded polyQ protein could be inhibited by peptides binding specifically to the expanded polyQ stretch, as Aβ aggregation was shown to be inhibited by Aβ binding peptides [23]. Furthermore specific recognition of the expanded polyQ stretch, but not normal one by a peptide seemed feasible,

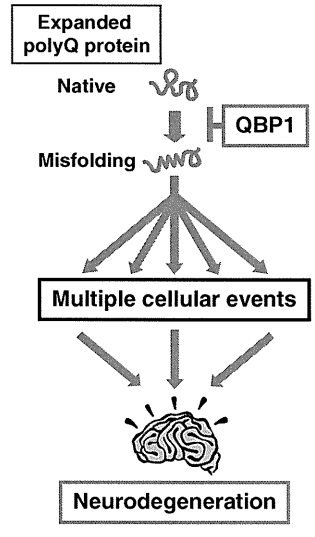

Fig. 1 Therapeutic target and effect of polyglutamine binding peptide 1 (QBP1). Proteins with an expanded polyglutamine (polyQ) stretch are prone to misfold, which then affects multiple cellular events, which will eventually lead to neurodegeneration. QBP1 inhibits the initial misfolding of the expanded polyQ protein, resulting in inhibition of a wide range of downstream pathogenic events and, hence, is able to suppress neurodegeneration

as a monoclonal antibody (1C2) was shown to bind selectively to expanded polyQ stretches, probably by detecting their unique structure [24]. We therefore screened for peptides that bind selectively to the expanded polyQ stretch by using the phage display technique [25]. Eleven amino acid combinatorial peptide libraries expressed on the surface of M13 phage were analyzed for their binding to a Q62 stretch by enzyme immunosorbent assay. The positive phage clones were then analyzed further for their selective binding to the expanded length Q62 compared with the normal length Q19. Six phage clones with greater binding affinity for Q62 compared with Q19 were identified, and the encoded peptide sequences were named polyQ binding peptide 1–6 (QBP1-6; Table 1). QBP1 (SNWKWWPGIFD), which showed the greatest differential binding affinity to the pathologic length polyQ compared with normal length polyQ, was chosen for further analysis.

We further characterized the binding properties of QBP1 to the expanded polyQ stretch by using the surface plasmon resonance technique. QBP1 was found to bind to Q62 with an equilibrium dissociation constant (K_d) of 5.7 μM, while it did not bind significantly to either Q0 nor Q19 [26]. A scrambled sequence of QBP1 (SCR; WPIWSKGNDWF), however, did not show any binding affinity to Q62. These results confirm the striking property of QBP1 to bind selectively to the expanded polyQ stretch, but not normal one probably by recognizing a conformation that is present only in the expanded polyQ stretch.

QBP1 Inhibits the Toxic Conformational Transition and Aggregation of the Expanded PolyQ Protein

We next tested the effect of QBP1 on the conformation of the expanded polyQ protein. Using circular dichroism analyses we demonstrated that QBP1 inhibits the initial β-sheet conformational transition of the expanded polyQ protein monomer [12] (Fig. 1; Table 2). Furthermore, we showed, by microinjection of different polyQ protein species into cultured cells, that this β-sheet conformational transition causes cytotoxicity. Recently, Carrion-Vazquez and colleagues [27] found that QBP1 reduces the frequency of mechanostable expanded polyQ protein monomers, presumably by preventing the β-sheet conformational transition (Table 2). To date, QBP1 is the only molecule that has been shown to selectively bind to the expanded polyQ stretch and inhibit its toxic β-sheet conformational transition.

We also tested whether QBP1 can inhibit the subsequent aggregation of the expanded polyQ protein using an *in vitro* assay that we designed previously [25]. In this assay, polyQ stretches fused with thioredoxin (thio-Qn) form aggregates *in vitro* in a time-, concentration-, and polyQ-length dependent manner (for polyQ >40), which mimics the expanded polyQ protein *in vivo*. We found that co-incubation of QBP1 with thio-Q62 dramatically inhibits thio-Q62 aggregation in a concentration-dependent manner, showing an almost complete inhibition at a stoichiometry of 3:1 (thio-Q62:QBP1) [25] (Table 2) . The control peptide SCR had no effect on thio-Q62 aggregation. Furthermore, addition of QBP1 after the initiation of thio-Q62 aggregation inhibited any further aggregation, but could not solubilize the aggregates that were already formed, confirming that QBP1 inhibits the earlier stages of the polyQ aggregation process [28]. We also found that $(QBP1)_2$, a tandem repeat of QBP1 (see Table 1) with a higher binding affinity to the expanded polyQ stretch (Kd 0.6 μM), presumably due to the additional polyQ binding sequence, exhibits stronger polyQ aggregation inhibitory activity [26]. These results demonstrate that aggregation inhibitory activity is determined by the binding affinity to the polyQ stretch.

Table 1 Polyglutamine binding peptides (QBPs) identified to bind preferentially to the expanded polyQ stretch

Name	Q62/Q19 binding ratio	Sequence (X_5-fixed-X_5)
QBP1	1.66	SNWKWWPGIFD
QBP2	1.31	HWWRSWYSDSV
QBP3	1.30	HEWHWWHQEAA
QBP4	1.27	WGLEHFAGNKR
QBP5	1.25	WWRANWATPVD
QBP6	1.23	WHNYFHWWQDT
$(QBP1)_2$	ND	SNWKWWPGIFDSNWKWWPGIFD

ND = not determined.

Therapeutic Effects of QBP1 on Cell Culture Models

We also examined whether QBP1 could exert therapeutic effects on cell culture models of the polyQ diseases [25]. We co-expressed QBP1 fused with cyan fluorescent protein (QBP1–CFP) together with an expanded polyQ stretch fused with yellow fluorescent protein (polyQ–YFP) in COS-7 cells, which resulted in colocalization of QBP1–CFP with polyQ–YFP inclusion bodies. Importantly, we found that QBP1–CFP inhibited polyQ–YFP-mediated cytotoxicity, as well as inclusion body formation, and its effect was stronger for shorter length polyQ stretches (Table 2). Furthermore, expression of $(QBP1)_2$–CFP had a more robust therapeutic effect than the single QBP1, which is in accordance with our *in vitro* results [26].

We also investigated the effect of QBP1 on oligomer formation of the expanded polyQ protein in cells, which

occurs before inclusion body formation, using fluorescence correlation spectroscopy and fluorescence resonance energy transfer. QBP1 decreased the amount of expanded polyQ protein oligomers, and the effect was greater for shorter length polyQ stretches [29, 30] (Table 2). These results are consistent with our *in vitro* data, which show that QBP1 inhibits the monomeric conformational transition of the polyQ protein that occurs before oligomer and aggregate formation.

Therapeutic Effects of QBP1 by Crossing of Transgenic Animals

As the next step towards developing QBP1 as a therapeutic molecule, we investigated whether overexpression of QBP1 can exert therapeutic effects *in vivo*. For these analyses we used *Drosophila* models of the polyQ diseases, as *Drosophila* are advantageous for various reasons, including their low cost, short lifespan, and ease of genetic manipulation [31]. Transgenic flies expressing an expanded polyQ protein under the control of an eye-specific promoter demonstrate degeneration of the eyes, as well as inclusion body formation, while flies expressing an expanded polyQ protein under a panneuronal promoter exhibit shortened lifespan due to neurodegeneration. Crossing of flies expressing $(QBP1)_2$–CFP and flies expressing the expanded polyQ protein in the eyes resulted in significant inhibition of eye degeneration, as well as inclusion body formation [32] (Table 2). Co-expression of $(SCR)_2$–CFP did not affect the polyQ-induced phenotype at all. Furthermore, crossing of $(QBP1)_2$–CFP-expressing flies with flies expressing the expanded polyQ protein in neurons resulted in a dramatic extension of lifespan. These results demonstrate clearly the therapeutic effect of QBP1 on polyQ-induced neurodegeneration *in vivo*.

Therapeutic Effects of QBP1 by Exogenous Delivery

Although our results demonstrate the effectiveness of QBP1 *in vivo*, to establish a therapy for the polyQ diseases using QBP1, QBP1 needs to be delivered to vulnerable neurons in the brain, rather than be expressed by the crossing of genetically-engineered animals. For this purpose we have attempted two methods: 1) delivery of the QBP1 transgene using viral vectors and 2) delivery of the QBP1 peptide using protein transduction domains (PTDs).

To deliver the QBP1 transgene into the brains of polyQ disease mice, we used adeno-associated virus vector (AAV) because of its widespread infection throughout the brain, its long-term expression of transgenes, and its safety [33]. Injection of AAV5–QBP1 into the brains of a polyQ disease mouse model resulted in significant inhibition of inclusion body formation (Table 2). However, we were unable to detect the therapeutic effect of AAV5–QBP1 on the neurologic phenotypes of these mice, such as motor impairment and shortened lifespan [34]. As the infection efficiency of AAV5–QBP1 was quite low (~30 %), the extent of neurons expressing QBP1 in the polyQ disease mouse brains was

Table 2 Summary of the effect of polyglutamine binding peptide 1 on polyglutamine (polyQ) disease models

Model/experiment	Phenotype	PolyQ protein	Ref.
In vitro			
Co-incubation	–	Toxic β-sheet transition ↓	[12]
		Aggregation↓	[25]
		Mechanostable monomers ↓	[27]
Cell culture			
Overexpression	Cytotoxicity ↓	Inclusion bodies ↓	[25]
		Oligomers ↓	[29, 30]
PTD-mediated delivery	Cytotoxicity ↓	Inclusion bodies ↓	[38]
Drosophila			
Overexpression by genetic crossing	Lifespan ↑	Inclusion bodies ↓	[32]
	Eye degeneration ↓		
PTD-mediated delivery	Lifespan ↑	Inclusion bodies ↓	[38]
Mouse			
AAV5-mediated delivery	No effect detected	Inclusion bodies ↓	[34]
AAV2-mediated delivery	Lifespan ↑	Inclusion bodies ↓	[35]
	Clasping ↓	Aggregation ↓	
PTD-mediated delivery	Body weight ↑	No effect detected	[39]

PTD = protein transduction domains; AAV = adeno-associated virus vector.

probably insufficient to exert a detectable effect on the phenotypes. In fact, Bauer et al. [35] demonstrated that AAV2-mediated delivery of QBP1 ameliorates the neurologic phenotypes of polyQ disease mice (Table 2). Towards developing viral vector-mediated delivery of the QBP1 transgene as a therapy, several issues, such as control of gene expression and delivery of the virus throughout the patient brain, are anticipated to be solved. Using a blood–brain barrier (BBB)-permeable virus vector, such as AAV9 [36], may help to overcome the brain delivery issue.

For administration of the QBP1 peptide, we utilized PTDs to enable the intracellular delivery of QBP1, which are peptide sequences that are capable of penetrating the cell membrane and entering cells, and can thereby deliver covalently-bound cargo molecules into cells [37, 38]. We found that PTD–QBP1 added to the culture medium was transduced efficiently into cultured cells, and inhibited polyQ-mediated cytotoxicity and inclusion body formation [39] (Table 2). Furthermore, administration of PTD–QBP1 to a *Drosophila* polyQ disease model by addition of the peptide into their food resulted in extension of lifespan and inhibition of inclusion body formation [39], indicating the effectiveness of this method *in vivo* (Table 2). We further tested our strategy in a mouse model of the polyQ diseases [40]. Intraperitoneal injections of PTD–QBP1 slightly ameliorated the body weight loss of polyQ disease mice, indicating a therapeutic effect (Table 2). Unfortunately, we were unable to detect any improvement in the motor phenotypes or any inhibition of neuronal inclusion body formation, probably because PTD–QBP1 does not efficiently cross the BBB in mice. Nevertheless, our studies indicate the potential of PTDs for the delivery of QBP1 to patient brains, and improvement of the BBB permeability of PTD–QBP1 should lead to its development as a potential therapy for the polyQ diseases. For this purpose, we are currently screening for PTDs with high BBB permeablility, which will, hopefully, enhance the brain delivery of QBP1.

Another approach we are currently taking is to design low molecular weight chemical analogues of QBP1 with high BBB permeability. Towards this goal we have identified the minimal active sequence of QBP1 (WKWWPGIF) [28], as well as its pharmacophores [41, 42]. We are currently working towards elucidating the structure of QBP1 when bound to the expanded polyQ stretch, which should further aid in the design of small chemical analogues of QBP1.

Effects of QBP1 on Other Neurodegenerative Disease-causing Proteins

As mentioned in the *Introduction*, β-sheet-rich amyloid aggregates are formed not only in the polyQ diseases, but also in many other neurodegenerative diseases, such as AD, PD, ALS, and the prion diseases. As QBP1 is thought to recognize the β-sheet structure of the expanded polyQ stretch, it may also recognize the toxic conformation of other neurodegenerative disease-causing proteins. Accordingly, Carrion-Vazquez and colleagues [27] tested the effect of QBP1 on other neurotoxic proteins, including mutant Aβ involved in AD and mutant α-synuclein involved in PD. Interestingly, they found that QBP1 was able to inhibit the aggregation and formation of highly mechanostable monomers of mutant α-synuclein, but not mutant Aβ. These results highlight the potential of QBP1 as a general therapeutic molecule for a wide range of neurodegenerative diseases, although QBP1 does not simply recognize any β-sheet structure, but appears to have sequence specificity. Indeed, it has been reported that an oligomer specific antibody can inhibit the toxicity of several neurotoxic proteins, including Aβ, α-synuclein, and polyQ [43], and (-)-epigallocatechin gallate can also inhibit the fibrillogenesis of these proteins [44, 45]. Although the mechanism remains unclear, these molecules, including QBP1, may recognize a unique conformation that is present in many neurotoxic proteins. In addition, QBP1 may not bind to normal proteins with β-sheet structures, as QBP1 has sequence specificity and β-sheets tend to be located within the core of proteins. It will be interesting to see in the future whether QBP1 can exert therapeutic effects against *in vivo* models of diseases, such as PD.

Concluding Remarks

Here we have reviewed our therapeutic strategy against the polyQ diseases using QBP1—a peptide that binds selectively to the expanded, but not normal, length polyQ stretch, probably by recognizing its unique conformation (Fig. 1). We have provided a large body of evidence on the potential of QBP1 as a therapeutic molecule, from its effect on polyQ misfolding/aggregation *in vitro* to its effect on polyQ-mediated neurodegeneration *in vivo* (Table 2).

Although our work has been focused on the polyQ diseases, our approach can also be applied to a broad range of neurodegenerative diseases caused by protein misfolding/aggregation, such as AD, PD, ALS, and the prion diseases. Indeed, various peptides/proteins that inhibit protein aggregation have been reported to exert therapeutic effects in cell culture and animal models of these diseases [46, 47]. Furthermore, the recent study by Carrion-Vazquez and colleagues [27] suggests that QBP1 may, in fact, have potential as a therapy also for at least some of these other protein misfolding diseases, such as PD. We hope that in the near future aggregation inhibitor-based drugs will be developed and bring relief to patients suffering from these currently intractable neurodegenerative diseases.